

AD-A189 718

METHODS FOR DETERMINING PARTICLE SIZE DISTRIBUTIONS
FROM NUCLEAR DETONATIONS(U) AIR FORCE INST OF TECH
WRIGHT-PATTERSON AFB OH C H FORE MAR 87

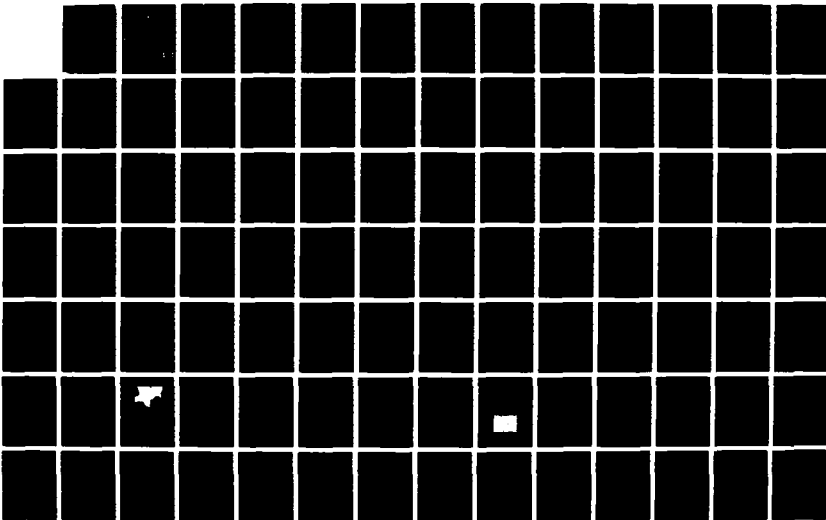
1/2

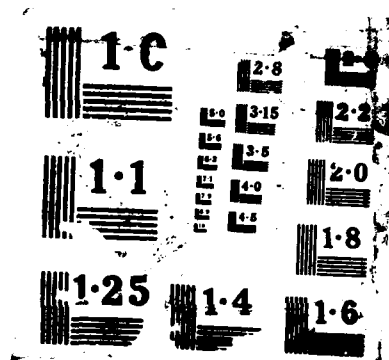
UNCLASSIFIED

AFIT/GNE/PH/87M-2

F/G 18/3

NL





DTIC FILE COPY

AD-A189 718



METHODS FOR DETERMINING
PARTICLE SIZE DISTRIBUTIONS FROM
NUCLEAR DETONATIONS

THESIS
Claude H. Fore, III
Captain, USA

AFIT/GNE/PH/87M-2

DTIC
SELECTE
MAR 07 1988
S OF H

DEPARTMENT OF THE AIR FORCE
AIR UNIVERSITY
AIR FORCE INSTITUTE OF TECHNOLOGY

Wright-Patterson Air Force Base, Ohio

DISTRIBUTION STATEMENT A

Approved for public release;
Distribution Unlimited

88 3 01 069

AFIT/GNE/PH/87

METHODS FOR DETERMINING
PARTICLE SIZE DISTRIBUTIONS FROM
NUCLEAR DETONATIONS

THESIS
Claude H. Fore, III
Captain, USA

AFIT/GNE/PH/87M-2

DTIC
ELECTE
MAR 07 1988
SH

Approved for public release; distribution unlimited.

AFIT/GNE/PH/87M-2

METHODS FOR DETERMINING
PARTICLE SIZE DISTRIBUTIONS FROM
NUCLEAR DETONATIONS

THESIS

Presented to the Faculty of the School of Engineering
of the Air Force Institute of Technology
Air University
in Partial Fulfillment of the
Requirements for the Degree of
Master of Science in Nuclear Science

Claude H. Fore, III, B.S.

Captain, USA

March 1987

Approved for public release; distribution unlimited

Preface

This thesis breaks the experimental ground, so to speak, in the area of particle size research at AFIT. The research was exploratory in nature and covered a wide range of methods. As with most theses, I didn't have enough time to do all the research and experimentation I wanted to do. However, I do feel that much was accomplished in this thesis, and, if nothing else, I have a strong indication of what does and does not work. I sincerely hope that this thesis will benefit future students, and that research in this area continues.

This thesis would have never gotten off the ground if it had not been for the guidance, encouragement and support I received from my thesis advisor, Dr. George John. To keep it flying and on course, I have many people to thank. First, I am especially grateful to Bob Hendricks and Don Smith for their laboratory support and guidance. Second, I would like to thank Sidney Childers of the Air Force Materials lab for supplying me with all the chemicals I needed. Third, I am most grateful to Dr. Robert Rundberg and his crew for their superb laboratory support at Los Alamos National Laboratory. Fourth, I am most appreciative for the help received from Ralph Omlor and William Anderson for their respective Transmission and Scanning Electron Microscopy Analysis of the samples. Finally, I would like to

express my heartfelt appreciation to my wife, Carla, not only for her support in processing this thesis, but also for her encouragement throughout this quarter.

----- Claude H. Fore, III
Captain, U.S. Army



Accession For	
NTIS GRA&I	<input checked="checked" type="checkbox"/>
DTIC TAB	<input type="checkbox"/>
Unannounced	<input type="checkbox"/>
Justification	
By	
Distribution/	
Availability Codes	
Dist	Avail and/or Special
A-1	

Table of Contents

	Page
Preface.	ii
List of Figures.	vi
List of Tables	vii
Abstract	ix
I. Introduction	1
Purpose	1
Background	1
Scope	2
Assumptions	3
Approach	3
Sequence of Presentation	4
II. Theory	6
General	6
Photon Correlation Spectroscopy (PCS)	6
Sedimentation Field-Flow Fractionation	11
Small-Angle X-Ray Scattering	22
Centrifugal Sedimentation	24
III. Equipment and Procedures	29
General	29
Sample Preparation	29
Photon Correlation Spectroscopy Analysis (Los Alamos)	34
Analysis by Vendors	39
IV. Results	41
General	41
Sample Preparation	41
Photon Correlation Spectroscopy Analysis (Los Alamos)	45
Results From Brookhaven Instrument Corporation Analysis (PCS)	52
Transmission Electron Microscopy	59
TEM Analysis of Sample R-6	59
TEM Analysis of Sample R-10	63
Samples R-3 and R-8	63
Comparison of Results	67

V.	Conclusions and Recommendations	69
	Conclusions	69
	Recommendations	72
Appendix A:	Alternate Method for Sample Preparation	74
Appendix B:	Particle Removal Procedure ("Sherill's" Method)	77
Appendix C:	Photon Correlation Spectroscopy Results	83
Appendix D:	Sedimentation Field-Flow Fractionation Results	84
Appendix E:	Abbreviations	85
	Bibliography	87
	Vita	89

List of Figures

Figure	Page
1. Schematic of PCS Equipment	7
2. Plot of Autocorrelation Function Versus Time	8
3. Schematic of SF ³ Equipment	12
4. Theory of SF ³	13
5. Plot of Reduced Layer Thickness Versus Reciprocal Field Strength for Various Particle Diameters	19
6. Retention Versus Particle Diameter	21
7. Elution Volume Versus Particle Diameter	21
8. Schematic of Centrifugal Sedimentation Equipment	25
9. Schematic of LTA Equipment	31
10. Particle Size Versus Cumulative Log Normal Probability for Sample R-3	57
11. Particle Size Versus Cumulative Log Normal Probability for Sample R-8	58
12. Sample of TEM Photograph	60
13. Particle Size Versus Cumulative Log Normal Probability for Sample R-6	62
14. Particle Size Versus Cumulative Log Normal Probability for Sample R-10	65
15. TEM Photograph of Sample R-8	66

List of Tables

Table	Page
I. PCS Evaluation	11
II. Evaluation of SF ³	23
III. Mass Estimate of Archive Sample Debris	30
IV. Summary of Sample Preparation Method	35
V. Set Parameters for PCS	39
VI. Analysis by Vendors	40
VII. Sample Weights	43
VIII. PCS Results from Unfiltered Samples	47
IX. PCS Results from Filtered Samples	48
X. Filtered Sample Summary	48
XI. Unfiltered Sample Summary	49
XII. Effective Diameters for Variable Angle Runs	50
XIII. GeLi Detector Results	51
XIV. Brookhaven Measurement Parameters for Samples R-3 and R-8	54
XV. Results From Brookhaven Analysis Using The Method of Cumulants	54
XVI. Results From Brookhaven Analysis of Sample R-3 Using Histogram Method	55
XVII. Results From Brookhaven Analysis of Sample R-8 Using Histogram Method	56
XVIII. TEM Particle Size Analysis for Sample R-6 . .	61
XIX. TEM Particle Size Analysis for Sample R-10 .	64
XX. Comparison of Results from Different Method Analyses	67


XXI. Benzene Rinse Results	76
XXII. Tabulation of Initial and Final Counts . . .	81
XXIII. Particle Removal Efficiency	82



Abstract

Samples were analyzed by ~~this~~ ^{author} using Photon Correlation Spectroscopy (PCS). The average diameter of the sample particles analyzed with this method ranged from 0.196 to 0.310 microns. Selected samples were also analyzed using Transmission Electron Microscopy (TEM). The data from these analyses were fit to a cumulative log normal distribution with mean diameters ranging from 0.160 to 0.217 and betas ranging from 0.61 to 0.77.

Finally, results received from a commercial vendor (Brookhaven Instruments Incorporated) who analyzed two samples using PCS indicate a bimodal distribution with mean particle diameter ranging from 0.296 to 0.298 microns with beta ranging from 0.37 to 0.75. The mean diameter for this analysis ranged from 0.198 to 0.350 microns.



METHODS FOR DETERMINING
PARTICLE SIZE DISTRIBUTIONS FROM
NUCLEAR DETONATIONS

I. Introduction

Purpose

The purpose of this thesis is to assess the potential of various methods for analyzing the sizes and distribution of particles produced by nuclear weapon detonations, and to briefly compare some of these methods with Transmission Electron Microscopy (TEM).

Background

Many studies of particle size distributions from nuclear detonations have been conducted since the first atomic bomb was exploded above the New Mexico desert. Experiments by Marcel Nathans and others have been done using Electron Microscopy as their primary tool for particle size analysis. In one of these studies Nathans found the particle size distribution to be log normal with median diameters between 0.5 and 1 micron (12:370). In order to keep larger particles from overshadowing the smaller ones when using an Electron Microscope, the particles first had to be size separated through centrifugation and filtering. These processes along with Electron Microscopy itself are very time consuming and tedious.

The samples to be analyzed were taken from a nuclear detonation, code-named Small Boy. According to E. C. Freiling who studied this shot considerably, Small Boy was radiochemically documented extensively (9:1). Therefore, a good radiochemical database exists for future radiochemical comparisons. Small Boy, a low-yield detonation, was exploded from a wooden platform slightly above the ground at the Nevada Test Site. Samples from this shot were collected in many places both in the air and on the ground. Air samples were taken between 15 and 120 minutes after detonation at altitudes between 15,000 and 16,700 feet. The particle sizes collected from this event ranged from 0.01 to 7.0 microns (12:305). However, most ranged from 0.1 to 0.2 microns (12:305). The particular sample received from the Los Alamos National Laboratory Archives was collected from an altitude of 15,000 feet at about 15 minutes after the detonation (19).

Scope

A literature search was conducted to find out what particle size analysis methods were feasible for this thesis. Four methods were selected from this list using the criteria that the method had to be able to analyze solutions with concentrations less than 100 parts per million, have a sample volume of 5 ml or less and be able to analyze particle diameters of 0.01 microns or greater. A technique for preparing samples from filter paper containing particles

collected from one nuclear detonation was then developed, and 13 samples were prepared using this technique. All 13 samples were analyzed using the Photon Correlation Spectroscopy Equipment (PCS) at Los Alamos National Laboratories. Four samples (R-6, R-10, R-3 and R-8) were analyzed using the Transmission Electron Microscopy Equipment at Wright-Patterson AFB and two samples were analyzed by 4 private companies (Brookhaven, Hiac/Royco, Dupont and Horiba) using 3 different methods (PCS, PCS, SF³ and Centrifugal Sedimentation respectively).

Assumptions

Since this thesis was exploratory in nature, only one assumption was made. It was assumed that the particles to be analyzed were approximately spherical. This assumption was necessary in order to easily obtain particle diameters and to discriminate between actual particles and other debris. The results from TEM indicate that this assumption is fairly accurate.

Approach

Initially, a comprehensive and somewhat exhaustive literature search was done to determine what particle size measurement methods could be used for particles originating from nuclear detonations. Each method was then analyzed against the following criteria:

1. Measurable range of particle sizes must include 0.01 to 1 micron.
2. Measurable concentrations must be at least as low as one hundred parts per million by weight.
3. Measurable sample volume must be 5 ml or less.

Out of this analysis, four possible methods were selected to be most feasible for this problem: Photon Correlation Spectroscopy (PCS), Centrifugal Sedimentation, Sedimentation Field Flow Fractionation (SF³) and Small Angle X-Ray Scattering. One brand of Photon Correlation Spectroscopy equipment was tested directly using the facilities at Los Alamos while other brands would be tested by various companies marketing their equipment. In addition, the same brand PCS equipment used at Los Alamos was also tested by the manufacturer to see if results received at Los Alamos could be duplicated. Centrifugal Sedimentation and Sedimentation Field-Flow Fractionation would also be tested by private companies. Small Angle X-Ray Scattering could not be tested for this thesis because facilities were not available.

Sequence of Presentation

Chapter II presents the theory of each method considered and is listed by method. The equipment and procedures

used not only for each method of analysis but also for the preparation of samples is discussed in Chapter III. The results for each method are contained in Chapter IV. Finally, any conclusions drawn from the results, as well as recommendations for further research are presented in Chapter V.

11. Theory

General

This chapter briefly describes the methods chosen for further evaluation and the theory of operation. These methods are presented in order of preference with the most probable selection being first. In addition to the basic theory, some of the advantages and disadvantages of each method are also discussed.

Photon Correlation Spectroscopy (PCS)

A Photon Correlation Spectroscopy system contains the following components (See Fig. 1): laser source, 2) sample cell, 3) Photomultiplier tube (PMT), and 4) autocorrelator. In PCS, light from the laser source is scattered from particles that are suspended in a clear liquid. This scattered light is then detected by the photomultiplier tube which can be oriented at various angles with respect to the incident laser beam. Since Brownian motion of these particles produces a time-dependent interference pattern, and since smaller particles diffuse faster than larger particles, the time-dependence of the interference pattern contains information about the particle size distribution. Specifically, an autocorrelation function ($C(\tau)$) measures the similarities between particle motion at one time and the same particles a short time later. This function is defined

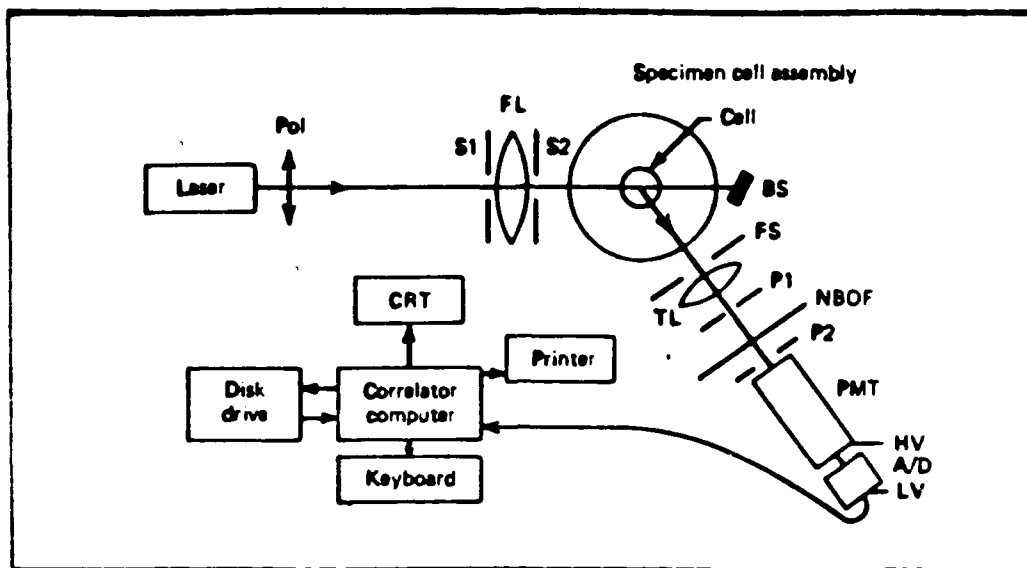


Fig. 1. Schematic of PCS Equipment (1:101).
For abbreviations see Appendix E.

as follows (5:2):

$$C(\tau) = \langle I(t)I(t+\tau) \rangle \quad (1)$$

where $I(t)$ and $I(t+\tau)$ are the respective intensities of scattered and laser light observed at time t and $t + \tau$. For particles that are monodisperse the autocorrelation function becomes (5:2):

$$C(\tau) = \langle I^2 \rangle [1 + b e^{-\Gamma \tau}] \quad (2)$$

where Γ is the time correlated spectrum decay constant, I is the intensity of scattered light, and b is an experimental constant. A plot of this function versus time is found in Figure 2. The decay constant, Γ , can be related to the

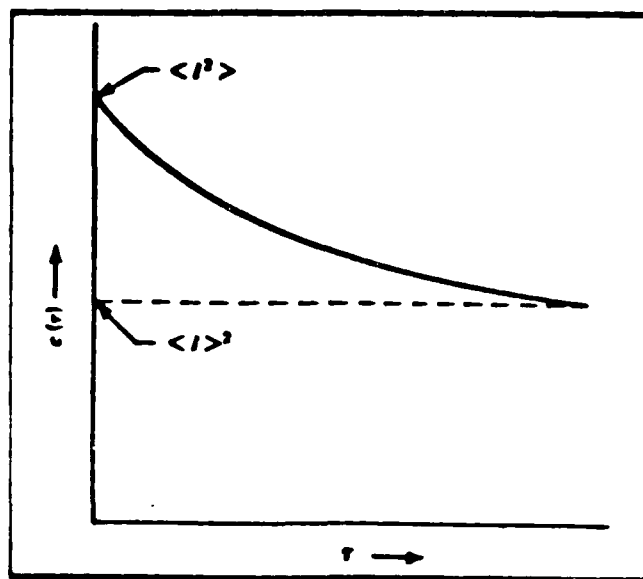


Fig. 2. Plot of Autocorrelation Function Versus Time (1:100).

diffusion of the particles through the following equation (4:2):

$$\Gamma = q^2 D \text{ (sec}^{-1}\text{)} \quad (3)$$

where D is the diffusion constant in m^2/sec and q is a factor relating to the equipment geometry by the following equation (5:2):

$$q = 4 \pi n \sin(\theta) / \lambda \text{ (m}^{-1}\text{)} \quad (4)$$

where n is the index of refraction of the suspending medium, and λ is the wavelength of the laser in a vacuum.

If the particles are spherical, their diameter, d , can be obtained from the diffusion constant, D , through the

Stokes-Einstein equation:

$$D = kT/(3\pi\eta d) \quad (5)$$

where k is the Boltzman's constant, T is the absolute temperature, and η is the viscosity of the solution. If the particles are not spherical then, d , would be the equivalent diameter for a spherical particle. By use of Eqs (2) through (5) the diameter of the particle can be determined from the autocorrelation function.

If the particles all have different sizes, (i.e. polydispersed), then the autocorrelation function equals the sum of exponentials weighted by the light intensity scattered from the particles of each characteristic size (5:2). A first order approximation of this function is as follows (1:109):

$$g^{(1)}(\tau) = \int G(\Gamma) \exp(-\Gamma \tau) d\Gamma \quad (6)$$

where $G(\Gamma)$ is the distribution function for the sizes of particles.

In order to get the distributions from Eq (6), the integral must be inverted, which is not easy to do. Robert Rundberg of Los Alamos National Labs is working on a program for deconvoluting Eq (6) to obtain particle size distributions from $g(\tau)$.

Other people have studied this problem and have developed methods for deconvoluting. The determination of

$G(r)$ from the measured correlation function $g(r)$ requires the inversion of the integral. This is made difficult because of the ill-conditioned nature of the inversion problems (21). Several different methods have been tried for obtaining $G(r)$. Provencher and Bott independently developed a method involving constrained regularization (2, 7).

Stock and Ray reference and present modifications of methods of constrained regularization developed by Provencher and Bott independently, and a method that uses non-negatively constrained linear least squares fit with data obtained at several scattering angles (26). Ostrowsky, et al have presented a method that uses eigenvalues and eigenfunctions of the Laplace transform to invert the integral (23). They also present references for other methods that have been tried, such as a semi-empirical approach that produces histograms of $G(r)$.

The advantages in using PCS are many. Only small sample quantities (less than 0.1% by weight) are needed and almost any suspending medium can be used, provided that it is not too viscous and relatively clear. In addition, no calibration is necessary for this method and broad distributions can be measured. Finally, PCS equipment is now commercially available at a relatively low cost (\$25,000) with measurement times from seconds to minutes.

There are a few disadvantages in using PCS,

especially for polydispersed samples. For one thing, measurements at more than one scattering angle would be required to obtain complete information about the particle size distribution. Secondly, this method generally does not produce a high resolution histogram of size distributions (1:113). Finally, this method is slightly sensitive to dust. Therefore, care would have to be taken in keeping dust out of the sample area. Table 1 contains an evaluation of PCS using additional criteria not listed in the Approach section.

TABLE I
PCS EVALUATION

Criteria	Evaluation
1. Small Concentration (<100 PPM)	Yes
2. Equipment Available	Yes
3. Reasonable Cost	Yes (\$25,000)
4. Can Measure Broad Distributions	Yes
5. High Resoluton for Polydispersed Particles	No

Sedimentation Field-Flow Fractionation (SF³)

Sedimentation Field-Flow Fractionation (SF³) is a fairly new method that uses a centrifugal field combined with fluid flow in a channel to separate particles into size groups. An ultracentrifuge is used to create this centrifugal field. The particles are injected at one end of a

long narrow channel that is fastened to the walls of an ultracentrifuge. The ultracentrifuge stratifies the particles. Then the particles are separated by a controlled laminar flow of the fluid in the channel. Separation occurs because the smaller and lighter particles are transported more quickly than the heavier particles. As the particles exit from the channel, they are detected by some method such as attenuation or scattered light. A schematic of this system is shown in Figure 3.

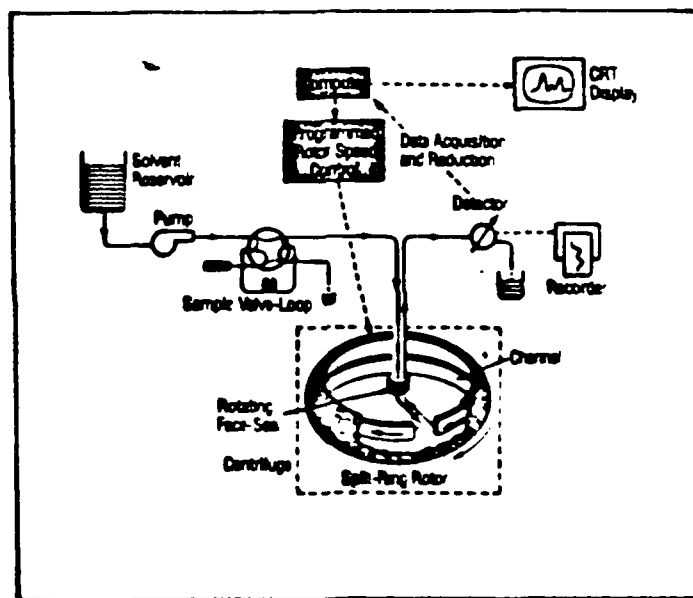


Fig. 3. Schematic of SF³ Equipment (18:1).

The details of this method are as follows: First the sample is injected into the channel followed by an initial liquid flow of water containing small amounts of surfactant, electrolyte or buffer solution. The flow is then stopped and a centrifugal field is applied perpendicular to the channel (See Figure 4). This field will stratify the

particles. The larger size groups will be closer to the wall of the container, while the groups of smaller size particles will be closer to the center of the chamber, due to Brownian motion.

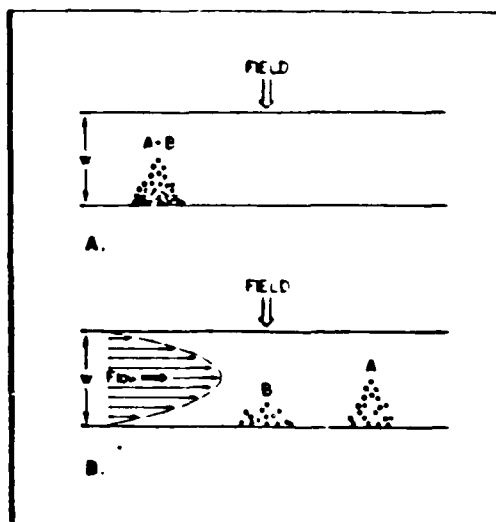


Fig. 4. Theory of SF_3 : (A) Prior to onset of flow, components a and b have reached their equilibrium distribution in the channel. (B) A laminar flow perpendicular to the field moves the two particle types downstream at different velocities (1:213).

When Brownian motion and the applied field are in equilibrium, the equation for the particle concentrations extending from the outer wall is as follows (1:214):

$$C(x) = C_0 \exp(-x/L) \quad (7)$$

where C_0 is the particle concentration at the outer wall, ($x=0$) and L is the layer thickness parameter defined in Eq (8). Here " x " is the location of the particle relative to the outer wall where $x=0$. This equation is only valid if the particle diameter is much less than L . The layer thickness

parameter can be related to the particle diffusion coefficient (D) in the following manner (1:214):

$$L = D/v \quad (8)$$

where v is the velocity of the particle due to the applied field, and can be related to the force of the field by the following equation:

$$v = F/f \quad (9)$$

where F is the force on the particle due to the applied field, and f is the frictional coefficient.

From the Einstein relationship an expression for the diffusion coefficient in terms of the frictional coefficient is found (1:214):

$$D = k T/f \quad (10)$$

where k is the Boltzman constant, and T is the absolute temperature. Substitution for v and D from Eqs (9), (10) into Eq (8) produces the following equation:

$$L = kT/F \quad (11)$$

A new parameter, reduced layer thickness (λ) is now introduced. The reduced layer thickness is just a ratio of the layer thickness parameter or particle zone to the width of the sample channel, i.e. (20:111):

$$\lambda = L/w \quad (12)$$

where w is the channel width.

After the field is applied and the particles are in equilibrium, the channel flow is restarted. This flow forces the particles to move in the same direction as the flow. The velocity for each particle zone is then calculated as follows (1:215):

$$v_{\text{ZONE}} = \langle v(x)C(x) \rangle / \langle C(x) \rangle \quad (13)$$

where $v(x)$ is the particle velocity as a function of x and $C(x)$ is the particle concentration. In other words, the velocity for each zone is taken as an average of all the particles in the zone.

For channels whose width is much less than its length the infinite parallel plate approximation for laminar flow can be used for $v(x)$ (14:34):

$$v(x) = 6\langle v \rangle (x/w - x^2/w^2) \quad (14)$$

where $\langle v \rangle$ is defined as the average linear velocity between the parallel plates of the channel with spacing w (1:215).

A retention factor, R , is defined as the ratio of the sample zone velocity to the velocity of the medium i.e. (1:278):

$$R = v_{\text{ZONE}} / \langle v \rangle \quad (15)$$

Since v_{ZONE} is less than $\langle v \rangle$, the range of values of the retention factor is $0 < R < 1$. Thus the heavier particles take

longer to exit from the channel and therefore have a smaller retention factor. The ratio of these two velocities, then, is the same as the ratio of the times for elution of "free" particles that travel at the speed of the fluid "retained" particles. These times are, in turn, directly proportional to the volume eluted, i.e. (1:215):

$$R = t^0/t_e = V^0/V_e \quad (16)$$

where t^0 and t_e are elution times for a free particle and a retained particle respectively, and V^0 and V_e are elution volumes for the same particles. It is the evaluation of these elution volumes that actually produces particle size results.

A relation for R can be obtained from Eqs (13), (14) and (15), after evaluating the expectation values (10:1917):

$$R = 6 \lambda [\coth(1/(2 \lambda)) - 2 \lambda] \quad (17)$$

For particles whose diameter is close to the particle layer thickness L , the following modified retention equation would apply (1:217):

$$R = 6b(a-a^2)+6 \lambda (1-2a)[\coth((1-2a)/2\lambda) - 2 \lambda / (1-2a)] \quad (18)$$

where $a=r/w$ and b is a velocity dependent factor close to unity and r is the particle radius. Steric conditions occur if a is much greater than λ . In this case Eq (18) would

simplify to:

$$R = 6ba \quad (19)$$

The equation for the force placed on the particles with this technique is as follows (1:220):

$$F = m'a = m(1-q/\rho)G \quad (20)$$

where m' is the total mass of the particle with the buoyancy of the medium taken into account, m is the total mass of the particle, q is the density of the liquid, ρ is the density of the particle and G represents the acceleration due to centrifugal forces. Combining Eq (11), (12), and (20) one arrives at the following equation for reduced layer thickness for SF^3 (1:220):

$$\lambda = kT/\{m(1-q/\rho)GW\} = kT/[(m(q-\rho)/\rho)GW] \quad (21)$$

where $q-\rho$ is the difference in density between the particles and the medium. If the particles are spherical, $m = d^3 \pi \rho /6$ and Eq (21) becomes (1:220):

$$\lambda = 6kT/(d^3 \pi (q-\rho)GW) \quad (22)$$

from which:

$$d = \{6kT/[\lambda \pi (q-\rho)GW]\}^{1/3} \quad (23)$$

Thus d can be determined when λ is obtained from the determination of R , the retention factor.

From Eq (21) one can see that there is an inverse relationship between λ and G . Thus for each group of particles with the same d the values of λ obtained for various values of G will produce a straight line when plotted against G^{-1} . The particle diameter can then be calculated from the slope (See Figure 5). However, if only the retention data is available at a fixed value of G , the particle diameter can be determined, if the density of the particle is determined first. One can find this density by varying the density of the carrier liquid provided that all particles eluted in a group have the same density.

Rewriting Eq (21) one gets:

$$1/\lambda = mGW/(kT) - mGWq/(\rho kT) \quad (24)$$

Now multiplying both sides by kT/GW and substituting m' for $(kT/(GW \lambda))$ one has (1:221):

$$m' = m - m/\rho q \quad (25)$$

Since the intercept of Eq (25) is the particle mass, a plot of the buoyancy adjusted particle mass (m') versus carrier fluid density (q) will reveal not only particle mass but particle density as well. Knowing these two values, one can find the particle diameter by using Eq (23).

Normally, the particle velocity is determined solely by the reduced layer thickness, λ , since the particle diameter is small compared to the thickness of the solute layer.

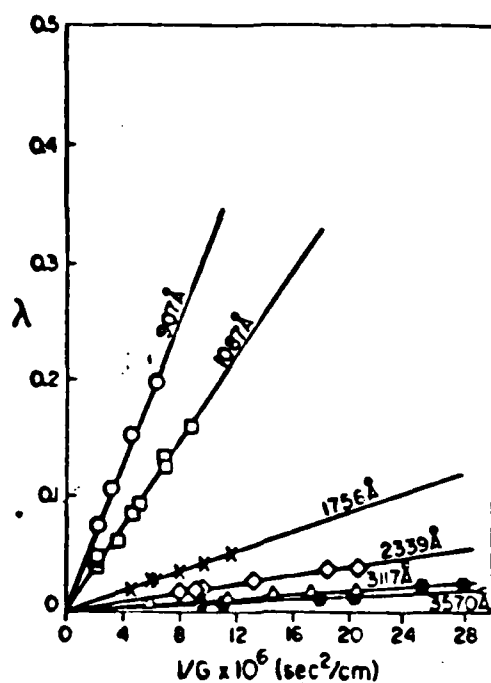


Fig. 5. Plot of Reduced Layer Thickness Versus Reciprocal Field Strength for Various Particle Diameters. The straight lines are obtained from Eq (21) (1:221).

However, if the particle diameter approaches or exceeds the solute layer thickness, then steric effects occurs.

As stated earlier, b in Eq (19) is velocity dependent. This factor depends upon, among others, frictional particle drag (1:234). When steric conditions apply, the particle diameter extends past one solute layer, into the faster layers. Thus once the centrifugal force is lifted, the normal channel flow causes the steric particles to experience a lifting force that draws them toward the faster middle solute layers. For this reason, in the steric region, larger particles move faster than the smaller

particles. With steric effects, the larger particles instead of the smaller ones elute first (1:233), and particle retention is determined by Eq (19).

As long as one stays exclusively in either the normal region or the steric region, accurate particle size distributions can be obtained. However, an intermediate or transition region exists between these two regions that can cause inaccurate results (See Figure 6). Fortunately, one can move this region up or down the particle size scale by varying either the centrifugal force or the density of the liquid. This becomes obvious as one examines Eq (22). Therefore, for broad distributions, one would have to vary either parameter to stay out of the transition region.

Since particle size is determined by the volume that elutes, one would reason that the best resolution is one where a small diameter difference would elute the largest volume. A plot of elution volume versus particle diameter for various centrifugal fields is shown in Figure 7. The peaks from these plots are the areas of best resolution for that particular field strength and that particular particle size. Naturally, one would want to consider this figure when choosing a field strength to use for this method, and two or more field strengths may have to be chosen for broad distributions.

SF³ has several disadvantages that may cause problems. This method will not work for concentrations

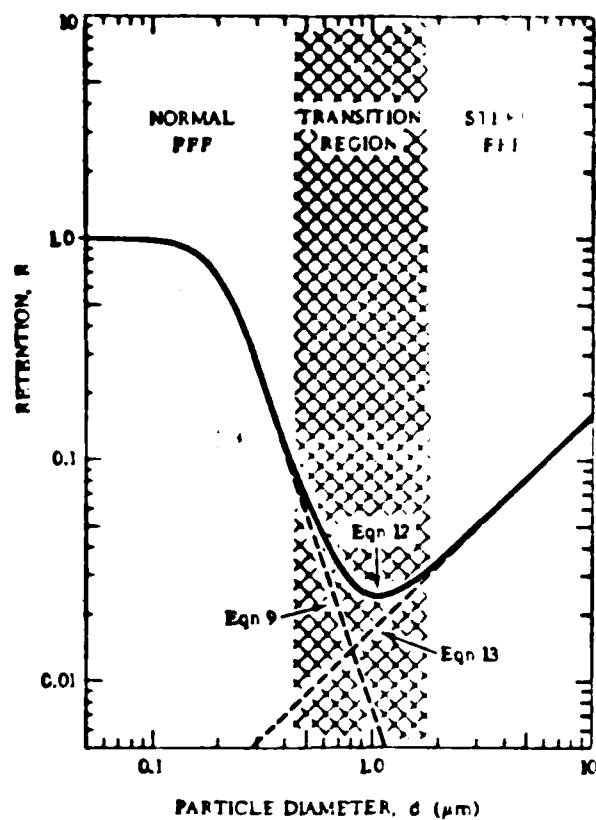


Fig. 6. Retention Versus Particle Diameter (1:224)

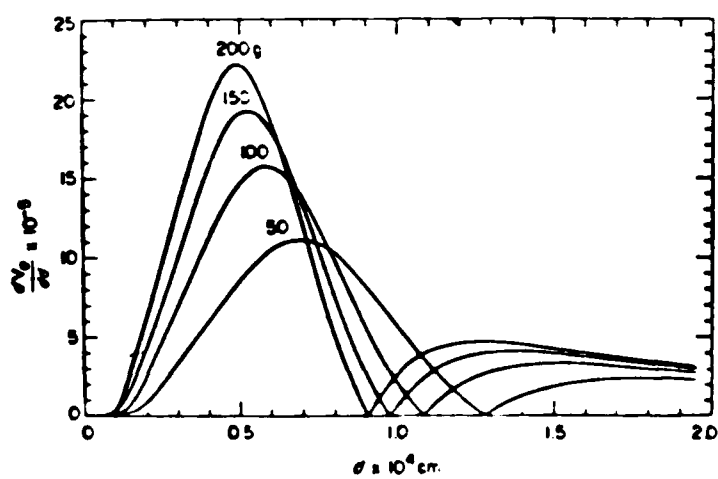


Fig. 7. Elution Volume Versus Particle Diameter (1:225).

below 0.1% by weight. This would be equal to about 1000 PPM. However since the sample volumes are extremely low (about 50 microliters), it is possible to achieve these required concentrations if some of the water in the samples is evaporated. A second disadvantage this method has is cost. This system uses an ultracentrifuge, which is expensive in itself, to achieve the necessary G forces. When the centrifuge is coupled to the other components needed for operation, the total cost comes to around \$90,000.00. Finally, this method is somewhat dependent on particle density. However, the method for determining this density that was discussed earlier would solve this problem provided the particle densities of these particles did not vary greatly.

There is one advantage SF³ has over PCS however. Since either the G forces or liquid density can be varied, this method has relatively good resolution for broad distributions. This advantage alone may overshadow the system's disadvantages. Table II provides a quick evaluation of this method.

Small Angle X-Ray Scattering

The Small Angle scattering of X-rays is being considered because it has the possible advantage of analyzing the particles while they are still on the filter paper. Unfortunately, the theory behind X-ray scattering is somewhat involved, and would require more time than this

TABLE II
EVALUATION OF SF³

Criteria	Evaluation
1. Small Concentration (<100 PPM)	No
2. Equipment Available	Yes
3. Reasonable Cost	No (\$90,000)
4. Can Measure Broad Distributions	Yes
5. High Resolution for Polydisperse Particles	Yes

author had in fully understanding it. However, what was learned about X-ray scattering during the short time allotted will be discussed in this section.

It was experimentally observed that below angles of two degrees a continuous scattering from small particles takes place without any type of diffraction occurring that normally is observed (13:3). It was also observed that this scattering occurs for particles that are ten to one hundred times the X-ray wavelength (13:3).

If one takes a single particle and bombards it with X-rays from a single direction, the interference pattern will vary with the scattering angle. At the same scattering angle as the incident ray, the scattering rays are all in phase with one another. However as the scattering angle increases, the scattering rays become more and more out of phase with each other, until all the scattering rays cancel

each other out. This phenomena occurs when (13:3):

$$2 \theta = \lambda / d \quad (26)$$

where λ is the x-ray wavelength, θ is the scattering angle, and d is the particle diameter.

If practical limits on the X-ray energy and scattering angle are 1 keV and 2 degrees (approximately 0.035 radians), then the upper limit of particle diameter measurable by X-ray scattering would be about 0.018 micron. Particles up to 1 micron would require energies of about 18 eV which would never penetrate the filter paper containing the particles. In addition, there may be a significant amount of silicon inherent in the filter paper itself. Filter paper is made from cotton which could absorb a significant amount of silicon from the soil. Since the particle to be analyzed may also contain silicon, it may be difficult to distinguish between the particle spectra and background caused by the silicon inherent in the filter paper. Therefore, it is highly doubtful that this method can be used for analyzing these samples.

Centrifugal Sedimentation

Centrifugal Sedimentation, as opposed to Gravitational Sedimentation uses centrifugal force rather than gravity in order to analyze smaller particles. Particles down to 0.01 microns can be analyzed using this method. A schematic of the equipment normally used for this method is



●

●

●

●

●

field (1:6). Therefore, for centrifugal sedimentation, the sedimentation coefficient, S , would be (1:6):

$$S = 1/w^2 r (dr/dt) = M/f \quad (28)$$

If the densities of both the particle and the suspending medium are known, then the following equation for the sedimentation coefficient can be used (1:6):

$$S = V(\rho - q)/f \quad (29)$$

where V and ρ are the volume and density of the particles respectively and q is the density of the suspending medium.

Since it is assumed that the particles produced by modern weapons are spherical, then Stokes law can be applied giving the frictional coefficient as follows (1:6):

$$f = 3 \pi \eta d \quad (30)$$

where η is the viscosity of the suspending liquid and d is the particle diameter.

From Eqs (28), (29) and (30), and the equation for the volume of a sphere one arrives at the following equation (1:11):

$$S = 1/(w^2 r) (dr/dt) = (\rho - q)d^2/(18 \eta) \quad (31)$$

Thus if the terminal velocity of the particle (dr/dt) is known (d), the diameter of the particle can be determined from S . However, since the particle terminal

velocity is not constant for Centrifugal Sedimentation the exact procedure for finding the particle size distribution based on it's terminal velocity is complex and beyond the scope of this thesis. More information on this method can be found in Reference 3. The terminal velocity of the particle can be obtained from the arrival time of these particles as they enter the detector area. Most centrifugal sedimentation equipment employs a light attenuation method for detection.

There are a number of disadvantages to this method that make it less desirable than the others. First and foremost, this method depends on particle density. A re-examination of Eq (31) reveals that if the particle density is not known then the particle diameters cannot be found. However, it is estimated that the particle densities for the samples used in this study vary between 3 and 4 g/cm³. If, in Eq (31), the particle velocity remained constant, then an increase in density of 1 g/cm³ would decrease the calculated particle diameter by a factor of about 1.2. Naturally, this problem becomes more pronounced for larger particles.

For example, if the estimated particle density was less than the actual density by 1 g/cm³, then particles which were actually 0.8 microns in diameter would be detected as having a diameter of almost 1.0 micron. In addition, not all the particles would have the same density. Therefore, whatever density difference there was between the particles

would result in a corresponding error in particle size determination.

A second disadvantage of this method is that for particles approaching whatever wavelength of light is used (normally somewhere between 0.4 and 0.7 microns), Mie Scattering principles as opposed to Rayleigh Scattering principles apply. In the Mie Scattering realm, light extinction cross sections vary greatly and are somewhat complex. Therefore, the particle diameter reported may be somewhat innaccurate for 0.4 to 0.7 micron particles.

Finally, as with Sedimentation Field Flow Fractionation a concentration of 0.1% by weight is needed for this method. However, unlike SF³, the sample volume for this method is about 2 ml. Therefore a concentration of 1000 PPM or 2 mg per sample cell is needed for any analysis. As can be seen from Table VII, only one sample, R-4, would have enough mass to qualify for this method.

The only advantage this method has over the other methods is that it is cheapest. The cost for this system is about \$24,000.

In view of the above disadvantages, it is highly doubtful that this method could be used by itself. However, a possibility exists for this method to be used in conjunction with PCS.

III. Equipment and Procedures

General

Description of the equipment and procedures used for this study is divided into two main phases: Sample Preparation and Sample Testing. The sample preparation phase is the same for all methods tested. The sample testing section of this thesis consists of three categories:

- (1) Direct measurements made by the author with a Photon Correlation Spectrometer at Los Alamos National Laboratory (LANL);
- (2) measurements made by Materials Lab by Transmission Electron Microscopy (TEM);
- and (3) measurements made by four vendors of equipment for measurement of particles: Hiac/Royco, Brookhaven, DuPont and Horiba.

Both Hiac/Royco and Brookhaven make PCS equipment. DuPont produces equipment that uses the Sedimentation Field Flow Fractionation Method and Horiba equipment uses the Centrifugal Sedimentation Method.

Sample Preparation

The sample received from Gordon Knobeloch of the Los

Alamos National Laboratory Archives was a section of filter paper, triangular in shape and measured approximately 34 square inches. Knobeloch did not know the amount of nuclear debris on the sample. However, an estimate of the amount was made by weighing the sample and a blank U-1 filter cut in the same size and shape as the archive sample. This blank filter paper was received from AFTAC (similar to the filter paper used for the actual sample). Assuming the filter papers were nearly identical, the difference in mass between the two samples should have given the approximate mass of the debris on the paper. Table III shows the results of these measurements.

TABLE III
MASS ESTIMATE OF ARCHIVE SAMPLE DEBRIS

Mass of Blank U-1 Sample:	2.4 g
Mass of Archive Sample:	2.6 g
Mass Estimate of Debris:	0.2 g

The activity of the sample was also crudely analyzed by attaching the sample directly to the face of a Lithium drifted Germanium diode detector. The activity originated primarily from Cesium 137 which was measured at 9.5×10^{-3} microcuries. In addition a check with a geiger counter indicated a number of hot spots as well as dead spots.

In addition to this sample, Knobeloch also sent what

he called 'background paper' which could be used to test out any technique before the actual sample was used. The paper contained particles in the atmosphere obtained at a time when negligible debris from weapon tests was present in the atmosphere.

All of the filters contained an oily substance called kronisol, (dibutoxy-ethyl-phthalate) which aids in particle collection. As will be seen later, kronisol removal proved to be a major obstacle with this thesis.

Approximately half of the archive filter paper was cut into 1/2 inch X 1/2 inch squares, and the scrim or backing was removed. Five of these squares were placed in a one inch diameter glass dish. Then five glass dishes with the 1/2 inch squares were placed in a Low Temperature Asher (LTA) for approximately four hours. A schematic of a Low Temperature Asher is shown in Figure 9.

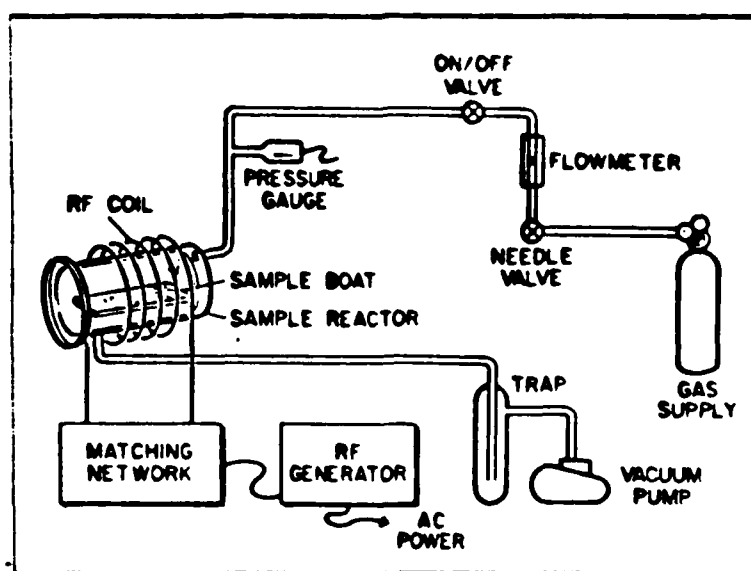


Fig. 9. Schematic of LTA Equipment (16:233).

A Low Temperature Asher uses an oxygen plasma to destroy organic material. Since the filter paper is made from organic material and the particles are inorganic, the Low Temperature Asher should destroy the filter paper leaving only particles. The oxygen plasma is created by pumping oxygen through a radio frequency coil. The radio frequency dissociates the oxygen molecule into monoatomic oxygen atoms and ions, thus creating an oxygen plasma.

Once the paper was ashed it was found that the residue adhered to the bottom of the container holding it. It is believed that kronisol caused this problem. Through experimentation, the best method found for removing most of this residue, containing both particles and the remaining ash, was to fill the glass dish holding the residue with acetone and place it in an ultrasonic cleaner for about six minutes. Even with this method, some residue (about 1-5%) still remained in the glass dish.

Once the residue was loosened from the glass dish, the particles had to be separated from the ash. It was assumed that the particles were primarily fused silicates with a density about 3 to 4 times that of water, while the ash had a density of a little greater than one. Therefore, if a liquid could be found that had a density between that of the ash and that of the particles, then the particles would sink to the bottom while the ash floated to the top, assuming there was no silica in the ash itself. However, as

stated earlier there may be a significant amount of silica in the filter paper and therefore in the ash also. A number of liquids could have been used but the one selected, primarily for safety reasons, was 1,1,1 Trichloroethane with a density of about 1.5.

A number of trials using a small portion of the blank U-1 filter and an optical microscope indicated that the 1,1,1 Trichloroethane did indeed cause the ash to float to the top. Therefore it was decided that after the acetone evaporated, the glass dish would be rinsed several times with 1,1,1 Trichloroethane into a glass vial until the vial was almost full. The rim of this vial was coated with teflon spray to repel liquid containing the ash and particles. Once the glass vial was filled with 1,1,1 Trichloroethane and shaken, small drops of this liquid were dropped onto the already full vial until a convex meniscus of liquid formed above the rim of the vial (NOTE: This meniscus would not have formed without the teflon coating). The protruding liquid with its surface-film of ash was then scraped off with a clean glass slide. It was hoped that this bulge contained most of the ash. However, as additional insurance (since the bulge was not very pronounced) about one milliliter of the liquid was pipetted off the top using the wide end of the pipette. Since the vial was shaken first the pipetted portion should have been representative of the entire mixture.

Once pipetted, the remaining mixture in the vial was poured into a 100 ml beaker to allow the 1,1,1 Trichloroethane to evaporate. A heat lamp was used to speed up the evaporation process. After evaporation approximately 5 ml of about 17 Meg-Ohm water was placed in the beaker. However it was found that the residue again adhered to the bottom of the beaker. As noted previously, this was probably caused by the kronisol. Therefore, the beaker was placed in an ultrasonic cleaner for about 3 minutes to loosen the residue.

Once the residue was loosened, the contents of the beaker was poured back into same vial used previously to separate the ash from particles. Then the beaker was rinsed three more times, each time with about 5 ml of 17 Meg-Ohm water. Therefore, the final product was a sample vial containing nuclear particles and other debris suspended in about 20 ml of water. A summary of the method just discussed is shown in Table IV.

Photon Correlation Spectroscopy Analysis (Los Alamos)

A twelve day trip to the Los Alamos National Laboratory INC-11 division (RadioChemistry Lab) was made to analyze the particle samples with the Photon Correlation Spectrometer. The specific equipment used was an Argon Laser, a Brookhaven Instrument Corporation autocorrelator, and an auxillary Digital computer system with an RLO2 hard disk. A schematic of the equipment set-up is shown in

TABLE IV

SUMMARY OF SAMPLE PREPARATION METHOD

1. Cut a 1/2 inch square from filter. Place in 1 inch O.D. glass dish.
2. Weigh glass dish and sample squares.
3. Place sample in LTA and ash for about four hours.
4. Half-fill glass dish with acetone, cover and place in ultrasonic cleaner for six minutes. Let acetone evaporate from dish.
5. Rinse glass dish several times with 1,1,1 Trichloroethane into a 25 ml glass vial previously coated with teflon until vial is almost full.
6. Shake.
7. Taking pipette, place a couple drops of TCE onto already full vial until a bulge forms on top of vial.
8. Scape off bulge with clean glass slide. Pipette about one ml of liquid using wide end of pipette. Pour liquid into 100 ml beaker and allow to evaporate.
9. Place 5 ml of triply distilled water in same 100 ml beaker, cover and place in ultrasonic cleaner for three minutes.
10. Pour contents of beaker back into glass vial. Rinse beaker three more times with 5 ml of triply distilled water each time.

NOTE: 1. Archive samples R-2 through R-12 were prepared by placing 5-1/2 inch filter squares in one glass dish each and placing 5 glass dish samples in the asher at one time.

Figure 1.

The digital computer analyzed the complex exponential produced by the autocorrelator by using the method of cumulants. The method of cumulants involved the expansion of the 1st order autocorrelation function equation (Eq 6) about the average linewidth, $\bar{\Gamma}$, using a MacLaurin Series. The result of this expansion is shown in the following equation (6:B-5):

$$\ln[b^{1/2}(g(m \Delta t))] = \ln b^{1/2} - \bar{\Gamma} (m \Delta t) + \frac{\mu_2 (m \Delta t)^2}{2} + \frac{\mu_3 (m \Delta t)^3}{3} + \dots \quad (32)$$

where μ_2 and μ_3 , etc. are moments of the linewidth distribution, b is an experimental constant, m is the channel number and Δt is the sample time.

Actually only the first two moments can be used from Eq (32), $\bar{\Gamma}$ and μ_2 . The 1st moment, $\bar{\Gamma}$, is related to the average diffusion constant, \bar{D} . In the same way Γ is related to D , i.e. (19:42):

$$\bar{\Gamma} = Dq^2 \quad (33)$$

In fact, the z-average or effective diameter is calculated from $\bar{\Gamma}$ in the same manner that a particle diameter is calculated from Γ .

The second moment, μ_2 gives the variance of the z-average diffusion coefficient distribution, i.e. (1:111):

$$\mu_2 = \overline{D^2} - (\bar{D})^2 \quad (34)$$

From this moment a polydispersity index, Q , is calculated according to the following equation (6:B-6):

$$Q = \overline{D^2} - (\bar{D})^2 / (\bar{D})^2 \quad (35)$$

Therefore, using the method of cumulants, PCS can only produce an effective diameter and a polydispersity index that measures the spread of the distribution as its main results.

In order to prepare the samples for PCS analysis, approximately 4 ml of solution was taken from each sample vial after the vial had been placed on a vortex machine for one minute and placed in an ultrasonic cleaner for four minutes. The solution was then placed in a 6 ml test tube for PCS analysis.

Sample analysis was relatively straight forward. The 6 ml test tube freed of dust by use of a jet of freon from an aerosol can was placed in the analysis chamber. Most of the input parameters remained the same for every sample analyzed. These parameters are shown in Table V. The only parameters that varied for each sample were sample time, Variable Optical Density Filter (VOD) setting that controlled the intensity of the laser beam, the aperture setting or the optical telescope that received the scattered light, and duration time. Sample time was adjusted until the bottom of the exponential curve from the correlator coincided with the bottom of the scale on the screen,

approximately three-quarters of the way across the screen. In this way, the measured baseline would coincide with the calculated baseline within a few percent. The VOD and aperture were set so that the scattered laser light would not overload the autocorrelator or the photomultiplier tube. Through experimentation it was found that the number of scattered photons varied proportionately with VOD setting, and a decrease in aperture setting by two created a fourfold decrease in photon count. The VOD setting controlled the intensity of the laser beam incident on the sample. Normally the VOD setting was set at 100 mV and the aperture ranged between from 50 to 200 microns. The duration time was normally set at 600 seconds for set angle (90 degrees) measurements, and 3000 seconds for variable angle (30-150 degree) measurements.

As mentioned above, two types of measurements were made. During the day, a series of three measurements were made at a fixed angle of 90 degrees. Then during the night a set of measurements was made at angles ranging from 30° to 150° in increments of 10°. The results from this set were collected the next morning. Every sample was measured at 90 degrees and selected samples were measured at various angles. These results are presented in the next chapter. The data from the measurements at various angles will be used for obtaining the particle-size distribution whenever the deconvolution program is developed by R.

TABLE V
SET PARAMETERS FOR PCS

Temperature:	298 K
Wavelength:	514.5 nm
Viscosity:	0.0089 Poise
Index of Refraction:	1.33

Rundberg (24). As it stands now, however, only the effective diameter and polydispersity can be presented.

Analysis by Vendors

As a further test of Photon Correlation Spectroscopy and to test the SF³ method, 5 ml of filtered and unfiltered samples were sent to private companies. Table VI lists the samples and companies involved along with the method tested. Results from these company tests are shown in the next chapter and in the Appendices.

TABLE VI
ANALYSIS BY VENDORS

Sample	Method Tested	Company
R-3	PCS	Brookhaven
R-8	PCS	Brookhaven
R-6	SF ³	Dupont
R-10	SF ³	Dupont
R-6	PCS	Hiac/Royco
R-10	PCS	Hiac/Royco
R-7	Cent. Sed	Horiba
R-11	Cent. Sed	Horiba

IV. Results

General

The final results of this thesis involved the evaluation of three different analysis methods: PCS, SF³ and Centrifugal Sedimentation along with a brief TEM analysis. PCS was evaluated not only first-hand but also by two other private companies, Brookhaven Instruments Corporation and Hiac/Royco Company. The results for the methods evaluated by two of the four private companies (Hiac/Royco (PCS) and Dupont (SF³)) have not been received at the time of this writing. Those results will be placed in the appendices as they are received. Therefore, only the results from the Los Alamos and Brookhaven PCS analysis and the TEM analysis will be presented in this chapter. Horiba, which analyzed selected samples using the centrifugal sedimentation method reported negative results.

In addition, since a major portion of the analysis problems have arisen from the sample preparation, a section on sample preparation is also included in this chapter.

Sample Preparation

Four types of samples were prepared by the same method: twelve archive samples (labeled R for real), four blank filter paper samples (labeled B), 5 practice paper samples (labeled PRP) and a scrim sample (labeled S). Most of the samples were weighed before and after ashing and

rinsing to determine the amount of debris left in the glass dish. A list of the samples prepared and their respective weights is shown in Table VII. As can be seen from this table the blank samples (except B-4) weighed very little after ashing. Some of the archive samples on the other hand weighed up to 2 mg after ashing. This result indicated that the ashing process was successful in eliminating most of the filter paper and leaving the particles behind.

A second result indicated from column 4 of Table VII is that for the most part the method described was successful in removing most of the residue from the glass dish. The cause for the increased weight of approximately 0.5 mg for the last three samples after rinsing is not known. However, the deviation is within the uncertainty observed by repetitive measurements with the analytical balance used for the measurements. Consequently, it is believed that the results show the method to be successful in removing residue from the glass dish.

The blank practice paper and the first archive sample (R-1) were made while the method in Table III was still being developed. Therefore a few anomalies occurred with some of the samples that need to be pointed out. First, the first ten samples listed in Table VII were prepared by placing one 1/2 inch filter square in a glass dish and ashing one at a time. Second, sample PRP-2 was destroyed when the glass dish broke while in the ultrasonic cleaner.

TABLE VII
SAMPLE WEIGHTS

Sample	Filtered (F) or Unfiltered (U)	Weight after Ashing (mg)	Wt. of residue left in glass dish after Rinsing (mg)
K-1	U	0.0	0.0
B-2	F	0.1	UNKNOWN
B-3	F	0.0	0.0
B-4	F	0.7	UNKNOWN
PRP-1	U	UNKNOWN	UNKNOWN
PRP-2	NA	0.7	UNKNOWN
PRP-3	F	0.8	UNKNOWN
PRP-4	F	0.8	UNKNOWN
PRP-5	F	0.0	UNKNOWN
R-1	F	UNKNOWN	UNKNOWN
R-2	F	UNKNOWN	0.0
R-3	F	1.8	0.1
R-4	U	2.1	0.0
R-5	F	1.1	0.0
R-6	F	1.4	0.0
R-7	F	1.7	0.0
R-8	U	0.5	0.0
R-9	U	0.7	0.0
R-10	U	0.2	0.1
R-11	U	0.5	0.5
R-12	U	0.4	0.6
S	U	2.0	0.9

Third, sample R-1 was rinsed with chloroform instead of acetone. As a result, long white fibers were produced in the sample. Fourth, sample R-4 did not ash completely. Finally, the cover from sample R-9 came loose while it was in the ultrasonic cleaner. This rendered the sample relatively useless since it had been contaminated. However sample R-9 was kept for analysis to see what results would be indicated.

Two major problems developed with this method that could not be entirely eliminated. The first already mentioned, was that some residue remained in each of the vessels used for sample preparation. It is assumed that some of the kronisol did not oxidize in the asher and remained as a residue in each vessel used. Probably some particles also adhered to the kronisol. The second major problem that occurred was that despite the two separation methods used, a significant amount of ash fibers remained in the sample vials. This became evident when examining the results of the Scanning Electron Microscope with some samples containing 0.05 micron polishing powder. This powder was placed on blank U-1 filter portion to test the method explained earlier. It was found that the powder granules were entangled in the ash fibers. In an attempt to eliminate this problem, various samples were filtered through a 3.0 micron millipore filter (See Table V). However, as seen in the next section of this thesis, filtering may eliminate

a significant portion of the particles themselves.

In another attempt to eliminate the kronisol problem, G. John (17) tried an alternate method of preparing the samples. A summary of this method is found in Appendix A. However, not enough time was available to produce significant results with this method.

Photon Correlation Spectroscopy Analysis (Los Alamos)

Results from the Los Alamos PCS analysis are listed in Tables VIII through XIV. All results (except for Table XIV) are averaged from a series of three or more 600 second runs. The average total counts in the tables have been normalized to those for an aperture setting of 50 microns and a VOD setting of 100 mV. Since the program for deconvoluting the sample spectrum had not been developed yet, only the effective diameter and polydispersity are available to analyze the spectrum. The effective diameter listed in these tables represents what should be the true diameter of the dry particle as opposed to the hydrodynamic diameter calculated from Stokes Law. It is calculated from \bar{F} in the same way the hydrodynamic diameter is calculated from Γ .

All results are calculated from the measured baseline. This is the recommended baseline for samples containing dust and other large debris. If the samples had been relatively free of debris the calculated baseline would have been a better choice.

The results of the PCS measurements of unfiltered

and filtered samples are summarized in Tables VIII and IX. In Table VIII (Unfiltered) the blank sample net and total counts are less than the archive sample net and total counts. This fact indicates that the background from the blank counts are not overshadowing the archive sample counts. However, in Table VIII (Filtered) this is not the case. In this table, most of the archive sample counts fall below the blank counts. Therefore, these two tables indicate that filtering the samples is a questionable procedure.

From Tables VIII and IX the ranges of effective diameter and polydispersity for unfiltered and filtered samples have been calculated and are listed in Tables X and XI respectively. Notice that for the unfiltered samples there appear to be particular groups that these different samples fall into. However, not enough unfiltered blank and practice samples were made to make a good determination. Therefore Tables X and XI indicate that PCS can discriminate between actual and blank samples.

Table XII lists results from the variable angle runs made on representative samples. These runs were made primarily for Rundberg to use with his deconvolution program, so that a complete particle size distribution could be created for each representative sample. However, one notices that samples B-2, R-1, R-2 and R-5 all follow a similar pattern in Table XII. That is, as the scattering angle is increased, the effective diameter decreases until

TABLE VIII

PCS RESULTS FROM UNFILTERED SAMPLES

Sample	Average Total Counts	Net Total Counts	Avg. Eff. Diameter (microns)	Average Polydispersity
B-1	2.84×10^6	1.22×10^3	1.02	0.375
PRP-1	2.27×10^6	789	0.759	0.322
R-4	8.04×10^6	2.10×10^3	0.675	0.277
R-8	1.74×10^7	3.49×10^3	0.290	0.275
R-9	2.08×10^7	4.05×10^3	0.279	0.275
R-10	1.85×10^8	1.11×10^4	0.220	0.262
R-11	2.69×10^7	5.51×10^3	0.310	0.292
R-12	6.96×10^7	1.23×10^4	0.245	0.232
S	9.38×10^5	366	1.08	0.630

Notes:

1. Average $d = 0.269$ micron
2. Results were averaged from three runs each. All results were within three standard deviations of mean.
3. Average Total Counts were normalized to AP=50 and VOD=100.
4. B = Blank, Filter PRP = Practice Paper Filter, R = Real or Archive Sample, S = Scrim
5. Results taken from measured baseline.

TABLE IX

PCS RESULTS FROM FILTERED SAMPLES

Sample	Average Total Counts	Net Average Counts	Avg. Eff. Diameter (microns)	Average Polydispersity
B-2	7.40×10^6	1.57×10^3	0.170	0.189
B-3	5.91×10^6	1.06×10^3	0.171	0.221
B-4	1.32×10^7	2.25×10^3	0.166	0.212
PRP-3	5.50×10^6	959	0.195	0.209
PRP-4	1.46×10^6	568	0.158	0.196
PRP-5	4.74×10^6	1.21×10^3	0.419	0.306
R-1	3.03×10^6	637	0.261	0.243
R-2	4.07×10^6	620	0.173	0.202
R-3	5.78×10^6	1.01×10^3	0.210	0.212
R-5	8.90×10^5	351	0.212	0.212
R-6	1.36×10^7	2.51×10^3	0.207	0.240
R-7	1.81×10^7	3.02×10^3	0.196	0.176

Note:

1. Average Total Counts are normalized to AP=5, VOD=100.

TABLE X

FILTERED SAMPLE SUMMARY

Sample	Eff. Diameter Range (microns)	Polydispersity Range
R	0.196-0.212	0.176-0.243
Blank	0.166-0.171	0.189-0.212
PRP	0.158-0.419	0.196-0.306

TABLE XI
UNFILTERED SAMPLE SUMMARY

Sample	Eff. Diameter Range (microns)	Polydispersity Range
R	0.220-0.310	0.232-0.292
Blank	1.02	0.375
Practice	0.759	0.322
Scrim	1.08	0.630

120 degrees is reached. Starting at 120 degrees, the effective mean diameter increases with increasing scattering angle. The unfiltered samples show no such pattern. This difference in sample patterns suggests that filtering the samples alters the original particle size distribution.

During the stay at Los Alamos, four unfiltered and three filtered samples were analyzed for Cs-137 using a well type Geli detector. The results from this analysis are listed in Table XIII. Notice that on an average case the unfiltered samples have twice as much activity as the filtered samples (120 vs. 61). It must be pointed out however, the filter and dish from sample R-2 had almost no activity also. Therefore, if sample R-2 is thrown out, then the filtered average is 103 counts. There is not enough data from filtered samples to make a determination. However, there is an indication that filtering does screen out some of the particles. This indication is further supported

TABLE XII

EFFECTIVE DIAMETERS FOR VARIABLE ANGLE RUNS

Angle	B-1*	B-2	PRP-1*	R-1	R-2	R-5	R-8*
30	1.050	0.329	0.969	0.385	0.355	0.349	0.523
40	1.000	0.281	0.824	0.349	0.282	0.291	0.430
50	1.000	0.244	0.791	0.327	0.250	0.262	0.381
60	0.916	0.216	0.849	0.307	0.228	0.237	0.327
70	0.879	0.196	0.807	0.294	0.211	0.222	0.305
80	1.020	0.180	0.835	0.275	0.187	0.200	0.291
90	1.200	0.170	0.882	0.269	0.172	0.198	0.287
100	0.987	0.159	0.797	0.253	0.163	0.187	0.288
110	1.000	0.154	0.941	0.246	0.158	0.181	0.301
120	0.843	0.157	0.683	0.250	0.163	0.198	0.323
130	1.030	0.162	0.772	0.256	0.166	0.213	0.360
140	2.090	0.176	1.570	0.251	0.197	0.246	0.532
150	5.150	0.195	4.770	0.319	0.209	0.414	0.748

* Unfiltered samples.

TABLE XIII
GeLi DETECTOR RESULTS

Sample	Average Area Counts	Average Percent
R-2(F)	3	NA
R-5(F)	79	33.4
R-7(F)	112	19.0
R-8	125	22.4
R-10	97	24.5
R-11	64	38.6
R-12	161	15.3
R-2 filter	6	NA
R-2 dish	17	NA
R-3 filter	101	26.1

F = Filtered sample

NA = Not Applicable

by the fact that the sample R-3 filter contained 101 counts. (It was discovered upon returning from Los Alamos that an analysis of sample R-3 itself was not done). It must be further pointed out that the archive filter (the filter that the R series samples were taken from) did not contain a homogeneous activity throughout. There were a number of hot spots and many dead spots indicated when a geiger counter was passed over it. Therefore, from the few samples analyzed no real findings can be made from this analysis.

One other observation was made with the PCS method itself. It appears that one needs to wait at least thirty

minutes after preparing the samples before analyzing them. Several test runs were made with unfiltered sample PRP-1 to see if shaking the sample had any effect. The results from three 600 second runs made immediately after shaking the samples were inaccurate since the difference between the calculated and measured baselines were over 10%. Since three 600 second runs total 30 at least thirty minutes it is recommended that analysis be delayed to at least thirty minutes after sample preparation.

There is also an indication that the results received from unfiltered samples may be dependent on the duration of settling time prior to analysis. It is known from the trial experiments with PRP-1 that one has to let the sample settle for at least thirty minutes before an analysis is done. However, time did not allow for any further experimentation. In addition, except as explained above, no note was made of the settling time involved for each sample. Therefore, it is not known whether longer settling times would produce different results or whether this phenomenon also occurs for filtered samples as well.

Results From Brookhaven Instrument Corporation Analysis (PCS)

Samples R-3 (unfiltered) and R-8 (filtered) were analyzed by the Brookhaven Instrument Corporation's BI-90 particle sizer. Nine measurements each were taken from samples R-8 and R-3 at a fixed angle of 90 degrees. Each

measurement consisted of 2500 cycles with each cycle lasting 500 nanoseconds. Before each measurement a short series of measurements were taken to get an average count. Any cycles containing counts above this average were rejected. The dust factors shown in the following Tables are the ratios of cycles rejected to total cycles for each run. In addition to the method of cumulants discussed earlier the BI-90 analysis sampler also uses the histogram method to compute a log normal distribution analysis.

A short summary of the histogram method is contained in an article by R. S. Stock and W. H. Ray (25:1399-1400). Measurement parameters for analysis of samples R-3 and R-8 are shown in Table XIV. Table XV shows the average results from the nine measurements taken for samples R-3 and R-8 using the method of cumulants. It is interesting to note that the results for sample R-8 for this analysis agree within 8 nm of the Los Alamos PCS analysis for the same sample (See Table VIII). However, the results for sample R-3 are different from the Los Alamos PCS results by about 80 nm. It is not known why there would be such a difference between results for sample R-3 and not for R-8. However it must be pointed out that an effective TEM analysis could not be done on either of these samples.

Results from the histogram method for samples R-3 and R-8 are shown in Tables XVI and XVII. Cumulative log normal distributions were plotted from this data and are

TABLE XIV
BROOKHAVEN MEASUREMENT PARAMETERS
FOR SAMPLES R-3 AND R-8

	Sample R-3	Sample R-8
Temperature	22.0 deg. C.	24.0 deg. C.
Viscosity	0.955 Centipoise	0.911 Centipoise
Ref. Index	1.332	1.332
Duration	2500 cycles	2500 cycles

TABLE XV
RESULTS FROM BROOKHAVEN ANALYSIS
USING THE METHOD OF CUMULANTS

	Sample R-3	Sample R-8
Effective Diameter	296 \pm 5nm	298 \pm 4nm
Polydispersity	0.277 \pm 0.007nm	0.257 \pm 0.012nm
Diff. Coefficient	1.53 $\cdot 10^{-6}$ cm ² /s	1.60 $\cdot 10^{-6}$ cm ² /s
Mol. Weight	0.36 g/mole	8.66 g/mole

shown in Figures 10 and 11. These results indicate a bi-modal distribution for both samples.

From Figure 10, the mean radius for the low mode for sample R-3 is about 0.21 microns and for the upper mode the mean radius is about 0.29 microns. The average standard deviation for the figure is ± 0.4 probits. The cumulative log normal plot for sample R-8 (See Fig. 11) indicates a low

TABLE XVI
RESULTS FROM BROOKHAVEN ANALYSIS OF
SAMPLE R-3 USING HISTOGRAM METHOD

Diameter (nm)	Cumulative Intensity (%)
138	12.0
161	26.0
188	40.0
219	55.0
256	71.0
298	88.0
348	90.0
406	90.0
474	90.0
553	90.0
645	90.0
752	90.0
877	93.0
1023	95.0
1194	96.0
1392	97.0
1624	99.0
1894	100.0

TABLE XVII
RESULTS FROM BROOKHAVEN ANALYSIS
OF SAMPLE R-8 USING HISTOGRAM METHOD

Diameter (nm)	Cumulative Intensity (%)
98	1.0
109	4.0
122	9.0
136	16.0
152	26.0
170	38.0
190	51.0
213	61.0
238	71.0
266	78.0
297	82.0
332	83.0
371	83.0
415	83.0
464	84.0
519	85.0
580	87.0
648	90.0
725	94.0
810	96.0
906	98.0
1012	99.0
1132	100.0
1265	100.0

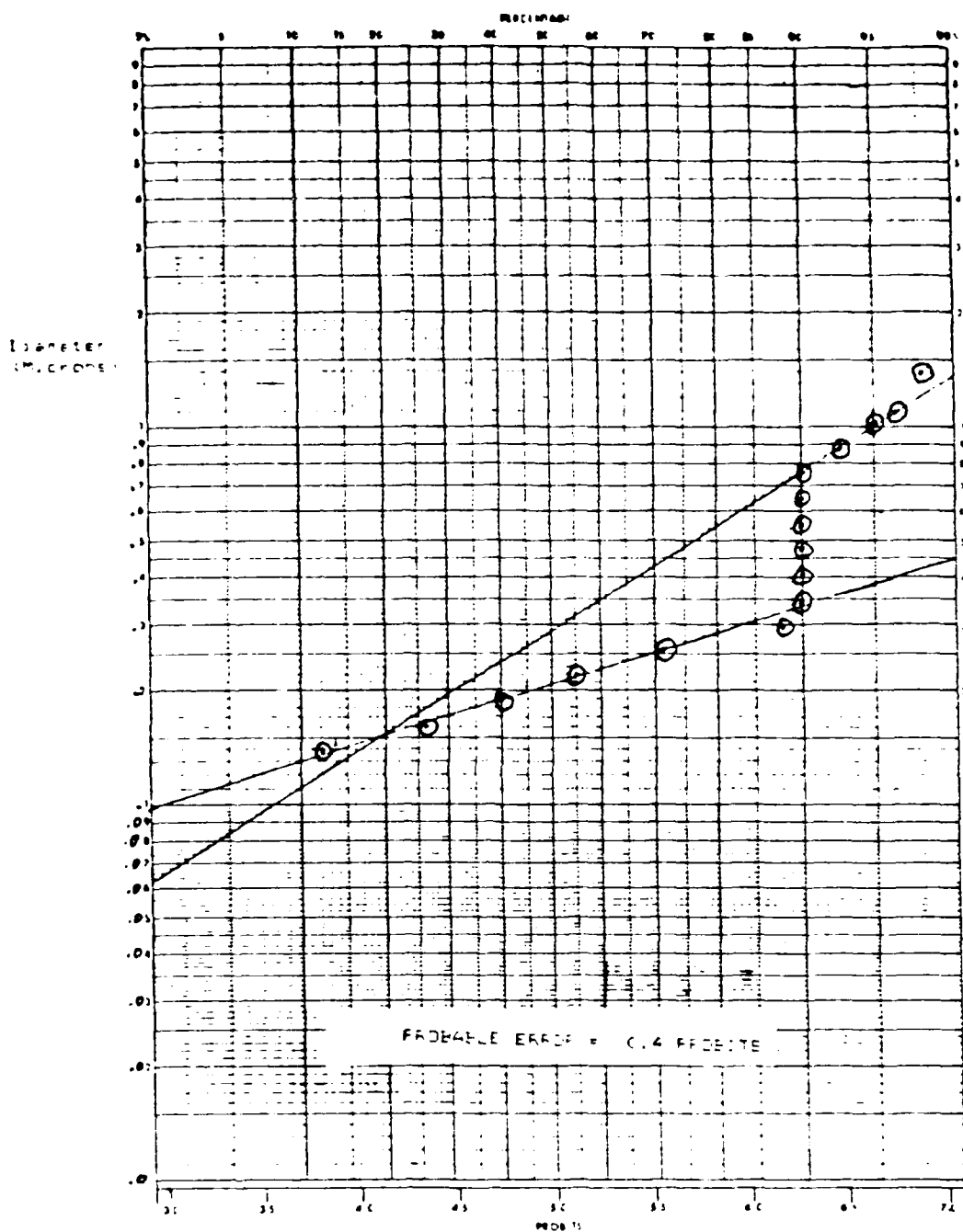


Figure 10. Particle Size Versus Cumulative Log Normal Probability for Sample R-3 (Based on Brookhaven PCS Analysis).

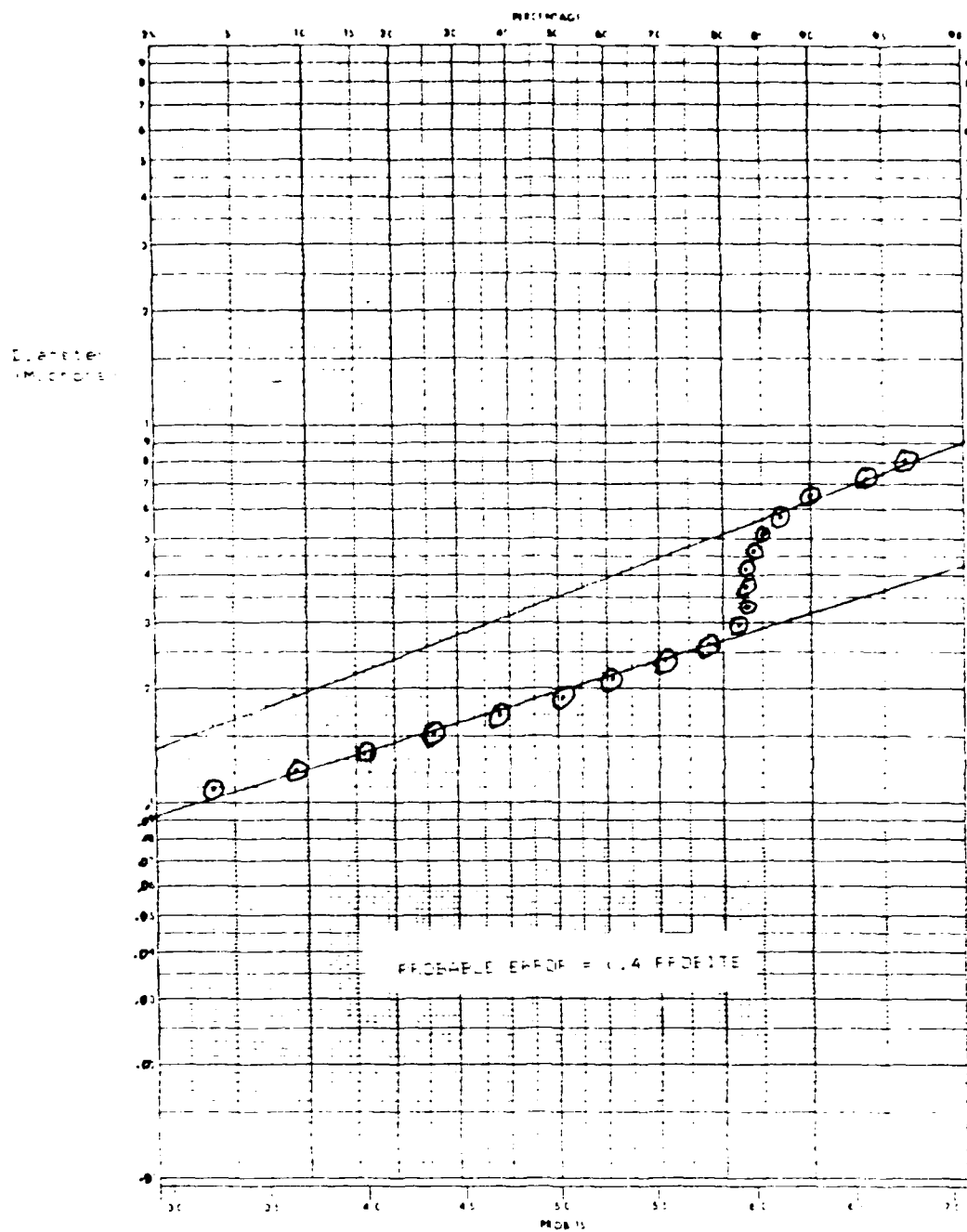


Figure 11. Particle Size Versus Cumulative Log Normal Probability For Sample R-8 (Based On Brookhaven PCS Analysis).

mode mean radius of about 0.20 microns and an upper mode mean radius of about 0.35 microns. The average standard deviation for this graph is ± 0.4 probits.

Since this analysis is the only one that indicates a binormal distribution and since no TEM analysis could be done on samples R-3 and R-8, it is not known how accurate this analysis is, especially since an 80 nm difference occurred between the two PCS analysis for the sample sample. Therefore, although there is some evidence for a bimodal distribution, this evidence cannot be weighed too heavily.

Transmission Electron Microscopy

Time allowed for only four samples, R-6 and R-3 (filtered), R-10 and R-8 (unfiltered), to be analyzed. A couple of drops from a sample were placed on a small copper grid coated with carbon for TEM analysis. From this analysis about ten negatives were made which appeared similar to the photograph shown in Figure 12.

Since it was assumed that the particles in these samples were spherical, the only particles measured in the negatives were the ones that were approximately spherical. This assumption may have been in error especially since in one study Nathans counted only those particles that were irregular in shape (12:367).

TEM Analysis of Sample R-6

One hundred thirty-seven particles were selected

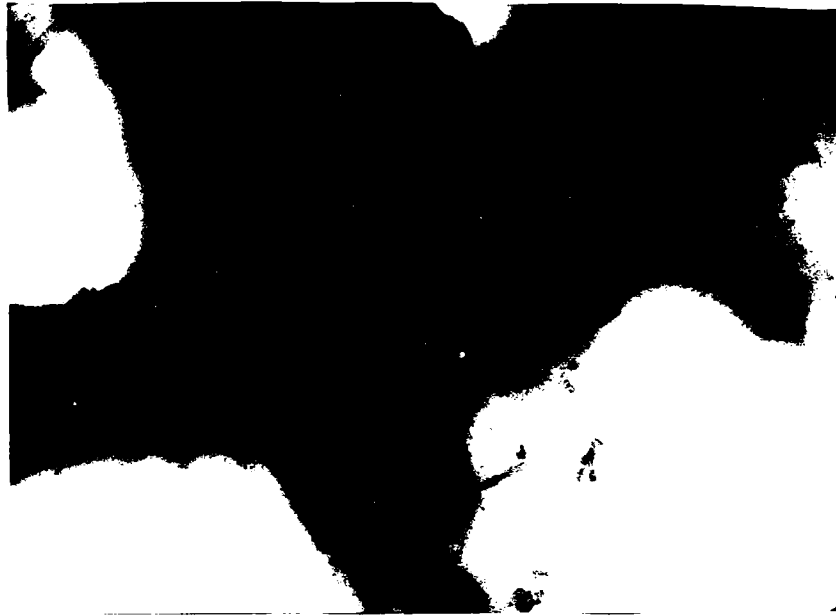


Fig. 12. Sample of TEM Photograph (Taken from TEM Analysis of R-6, Scale: 1mm = 0.02 microns).

from these negatives for particle size analysis. Table XVIII shows the results from this analysis.

From Figure 12, it is noticed that many of the particles are clinging to what appears to be a fiber. This observation seems to confirm what was already suggested from the PCS results. Interestingly enough, these fibers showed up in a sample filtered with a 3.0 micron filter. Therefore some of the fibers must be smaller than three microns.

The particle diameters listed in Table XVIII range from 0.02 to 1.10 microns, with most of the particle diameters falling between 0.1 and 0.2 microns. In addition

TABLE XVIII
TEM PARTICLE SIZE ANALYSIS
FOR SAMPLE R-6

Diameter (microns)	Frequency	Diameter (microns)	Frequency
0.02	2	0.18	5
0.03	4	0.19	3
0.05	2	0.20	3
0.06	10	0.21	3
0.08	8	0.22	1
0.09	7	0.23	1
0.10	9	0.25	5
0.11	7	0.27	1
0.12	15	0.30	4
0.13	11	0.34	1
0.14	4	0.35	2
0.15	12	0.40	4
0.16	7	0.42	1
0.17	5	0.44	1
		1.10	1

data from Table XVI was plotted on a Log Normal Cumulative Probability Graph shown in Figure 13 using an interval of 0.0275 microns. If the data in Table XIV were indeed log normal, then the data in Figure 13 should form a straight line. Indeed, it does appear that within statistical

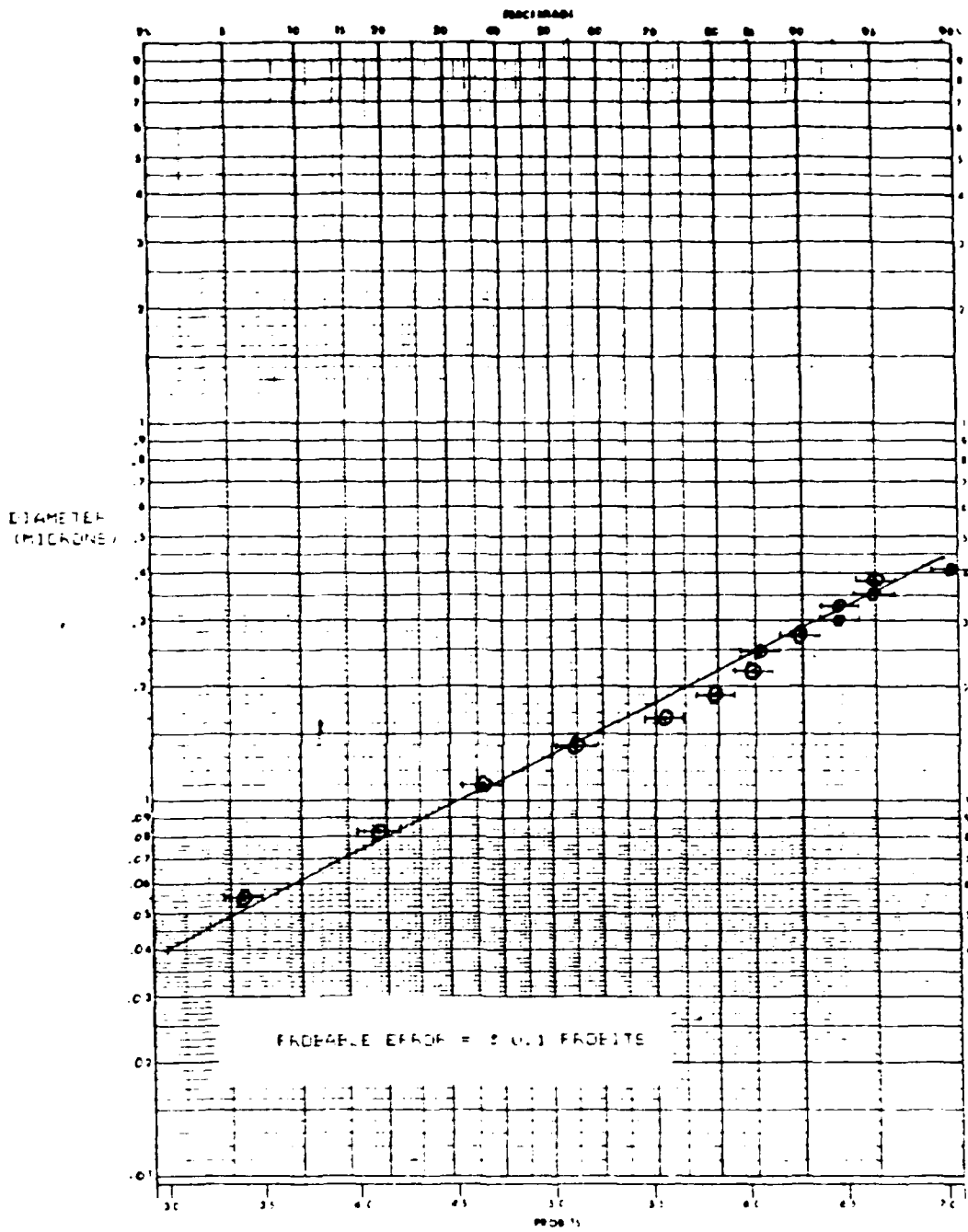


Fig. 13. Particle Size Versus Cumulative Log Normal Probability for Sample R-6 (Based on TEM Analysis).

variations a straight line is indicated in Figure 13. From the straight line plotted a median diameter of about 0.13 microns was found. A least squares fit (11:102-103) was used to fit the data to a straight line. The standard deviation for this figure determined using Bevington's method (3:93), was calculated as ± 0.1 probits.

TEM Analysis Of Sample R-10

Eighty-three particles were selected from eleven negatives for particle size analysis. Table XIX shows the results from this analysis.

The particle diameter listed in Table XIX range from 0.03 to 0.91 microns. Data from this table was plotted on a log normal cumulative probability graph shown in Figure 14 using an interval of 0.055 microns. Within statistical variations this data fits a straight line which indicates a log normal distribution. From this graph a median diameter of about 0.16 microns was found. The standard deviation for this graph was calculated to be ± 0.1 using the same method as for sample R-6.

Samples R-3 and R-8

A TEM analysis was attempted with samples R-3 and R-8. However, all the negatives received from this analysis were similar to Figure 15. Since an initial assumption was made that all the particles are spherical, no real analysis could be made from the TEM negatives received. It

TABLE XIX

TEM PARTICLE SIZE ANALYSIS FOR SAMPLE R-10

Diameter (microns)	Frequency	Diameter (microns)	Frequency
0.03	1	0.23	3
0.04	1	0.25	2
0.05	3	0.26	1
0.06	4	0.27	3
0.08	7	0.29	2
0.09	2	0.31	2
0.10	7	0.32	1
0.11	3	0.35	2
0.12	1	0.40	3
0.13	1	0.42	1
0.14	2	0.47	1
0.15	12	0.54	1
0.16	1	0.59	1
0.17	2	0.63	1
0.19	3	0.65	1
0.20	1	0.69	1
0.21	2	0.77	1
0.22	2	0.91	1

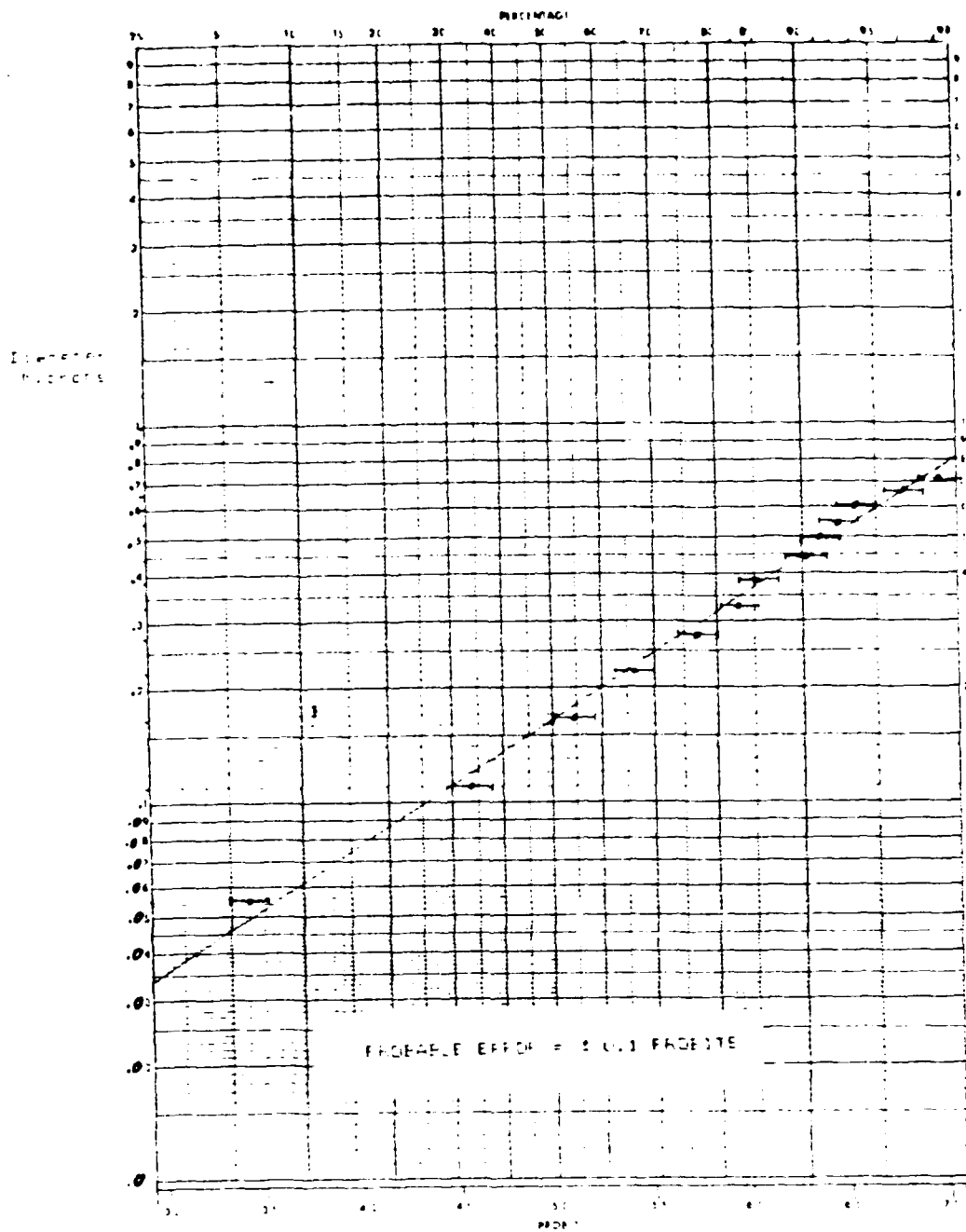


Fig. 14. Particle Size Versus Cumulative Log Normal Probability For Sample R-10 (Based On TEM Analysis).

is not certain why these samples appear different from samples R-6 and R-10. It was first thought that the particles had agglomerated in samples R-3 and R-8 before a TEM analysis was done, especially since a week had elapsed between the time the samples were ultrasonerated and the time they were analyzed. However, a second analysis was tried with only two days difference between ultrasoneration and analysis. This analysis revealed the same results as the first. It is now thought that perhaps there are too many particles in these samples for them to be separated effectively with ultrasoneration. Supporting this hypothesis is the fact that samples R-3 and R-8 did contain more mass after ashing than samples R-6 and R-10 (See Table VII).

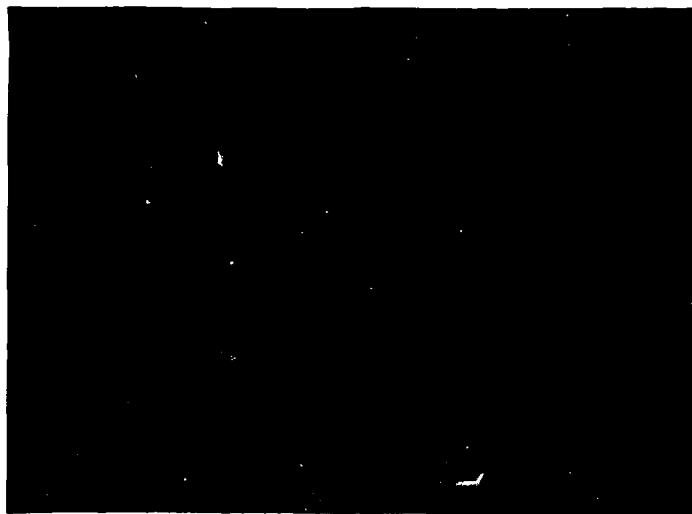


Fig. 15. TEM Photograph of Sample R-8.
(Scale: 1mm = 0.1 microns)

Comparison of Results

Table XX compares results received from the different methods. Beta was computed from the Brookhaven PCS data using the following formula:

$$\text{beta} = 1/2(2.054) \ln \{ r(98\%)/r(2\%) \} \quad (36)$$

where r = particle radius.

TABLE XX
COMPARISON OF RESULTS FROM
DIFFERENT METHOD ANALYSES

Sample	Method	Mean Diameter (microns)	Polydispersity	Median Diameter (microns)	Beta
R-3 (Filt.)	LPCS	0.210	0.212	NA	NA
	BPCS	0.296	0.277	0.288(U) 0.207(L)	0.75(U) 0.37(L)
R-8 (Unf.)	LPCS	0.290	0.275	NA	NA
	BPCS	0.298	0.257	0.350(U) 0.198(L)	0.46(U) 0.37(L)
R-6 (Filt.)	TEM	0.160	NA	0.123	0.61
	LPCS	0.207	0.240	NA	NA
R-10 (Unf.)	TEM	0.217	NA	0.15	0.77
	LPCS	0.220	0.262	NA	NA

LPCS = Los Alamos PCS Analysis

BPCS = Brookhaven PCS Analysis

(U) = Upper Mode

(L) = Lower Mode

NA = Not Applicable

(Filt.) = Filtered Sample

(Unf.) = Unfiltered Sample

It is seen from Table XX that for the two unfiltered samples (R-8 and R-10) the average diameter between the Los Alamos PCS and the Brookhaven PCS analysis differ by only 8 nm, and between TEM and Los Alamos PCS the difference is only 3 nm. However for the unfiltered samples (R-3 and R-6) the difference is 80 and 40 nm respectively. In addition, the difference in polydispersity between Los Alamos PCS and Brookhaven PCS is greater for the filtered (R-3) than for the unfiltered. It is not known why there is such a great difference between the different methods for the filtered samples and not for the unfiltered samples.

V. Conclusions and Recommendations

Conclusions

Although a number of problems occurred during this study, a number of conclusions can be made. It appears from Table V that the primary method for sample preparation is successful in removing most of the particles from the filter paper. Except for the last three archive samples, at least 95% of the particle weight was removed from the glass dish. However, due to the kronisol present in the samples, a visible residue remains on each vessel used to prepare the sample despite many efforts to free it. It is not known what percentage of the total particle population this represents. However, since this residue is visible as a thin film on each vessel and at least three vessels are used in the sample preparation, it is probably a significant amount.

A way around this problem may be to use the alternate method tried by John with the modification that whatever residue is left is ashed for an hour or so in an attempt to remove any fibers left. This technique, if successful, would not only remove the kronisol present, but would also eliminate any fibers that have plagued past experiments.

Tables X and XI indicate that there are bands or zones that the archive and blank samples fall into. This would indicate that PCS can at least distinguish between

blank and actual samples.

However, the analysis of effective diameter versus total counts and polydispersity for both unfiltered and filtered samples (Table XII and XIII respectively) indicate problems occur when the samples are filtered. This indication appears to be supported by the variable angle analysis (Table XIV). Therefore, it appears that filtering the samples actually removes some of the particle themselves. From the TEM photographs one can see that in fact, some of the particles cling to the filter fibers themselves. Therefore, when the sample is filtered, the fibers along with some of the particles themselves are taken out. Apparently enough of the particles are removed to alter the particle size distribution of the sample.

Another possibility is that there are actual particles larger than three microns in the samples. If that were so, then filtering with a three micron filter would screen out those particles larger than three microns, and thus alter the size distribution. In any case, it appears that the samples should not be filtered.

On the other hand, if the sample is left unfiltered, PCS analysis indicates the presence of large (greater than 1 micron) particles in the sample if the sample is analyzed before a settling time of 30 minutes is achieved. In addition, it is extremely hard to get the calculated and measured baseline to coincide within 10% unless the

unfiltered sample is allowed to settle for at least 30 minutes. It is not known for sure however, if the filter fibers are causing this problem or if there are actually particles greater than 1 micron present in the sample. Since the sample particle range for the Small Boy shot was from 0.1 to 7 microns (See Background Section), both the fibers and large particles may be causing this problem. One thing certain, however: more experimentation is needed in this area.

In order to determine whether or not the fibers are causing these large diameter PCS results, one should do a comparison of a number of unfiltered blank samples with some unfiltered archive samples. If the same problem occurred for both samples one can probably conclude that the fibers are causing the problem. If large diameter results occur for the archive sample but not the blank sample, then there probably are large particles in the archive sample itself.

It can be concluded from TEM analysis that the samples appear to fit a log normal distribution (See Fig. 13 and 14). In all cases the data fit a straight line to within two standard deviations and most fit within one standard deviation. In addition, there is a slight amount of evidence from the results of the Brookhaven PCS analysis (See Figs. 10 and 11) that the particles actually fit a bimodal distribution. However, no other results have indicated a bimodal distribution and no significant particles

could be resolved from the TEM analysis of the same samples analyzed by Brookhaven.

Finally since results from two company analyses (Dupont, and Hiac/Royco) have not been received, no final conclusions can be made as to which method is the best one for analyzing these particles. However, from the results received so far, it appears that TEM analysis is better than the other methods simply because with this method the particles can actually be photographed and counted by hand. Although somewhat tedious (1000 particles would have to be counted in order to get a good representative sample) this is the only method, that gives results that do not have to be compared to other results for accuracy. However, from the last attempted analysis of samples R-3 and R-8 even this method appears to have some unresolved problems. It may be that the TEM method will only be able to analyze samples below a certain concentration, or that samples would have to be filtered to screen out the larger particles. Since samples R-3 and R-8 were the only samples that could not be analyzed effectively more samples would have to be analyzed with TEM before a definite conclusion can be made. One thing is certain, however: more research will have to be done before the best method for analysis can be determined.

Recommendations

The biggest problem with this research is that not

enough unfiltered samples were prepared for analysis. In light of this it is recommended that a equal number of unfiltered and filtered samples be prepared and analyzed using PCS equipment. This analysis should include both set angles and variable angle. In addition, variable angle runs should be done on unfiltered archive samples not analyzed previously. Also recommend that unfiltered and filtered samples (along with their filters) be neutron activated and analyzed with a well-type GeLi detector to provide additional radionuclide activity data. All of these additional analyses would provide additional data to either support or refute the conclusions presented previously.

It is further recommended that the alternate method for sample preparation be reviewed and experimented with. Not enough time was available at Los Alamos to adequately experiment with this method, and it could solve a problem with this thesis, i.e. the adhesion of the residue to the containers due to kronisol. Particular attention should be focused on ashing the remaining fibers.

Appendix A: Alternate Method for Sample Preparation

While at Los Alamos National Laboratory, G. John learned of a method for removing particles from filter paper without using a low temperature asher. Allan Mason, a scientific associate at the Radiochemistry Lab gave John a copy of a method (herein called Sherill's method) developed by a doctoral student of his. This method was successfully used on U-1 filters taken from the Minor Scale Test. This test used a large amount of high explosives to simulate a nuclear blast.

The method developed by this student involves the removal of kronisol through successive soakings and decontations in Benzene. These Benzene rinses were saved and later centrifuged to recover any particles lost in the rinse. After the Benzene treatment, the filter paper is treated with "Freon" TE-35 and an ultrasonic probe to remove the remaining particles from the filter paper. Freon TE-35 is a mixture of 65% trichloro-trifluoroethane and 35% ethanol by weight. After the particles are ultrasonically "shaken" from the filter paper, the mixture is filtered through a 200 mesh screen.

As stated earlier, Sherill's method was developed mainly for the Minor Scale shot which was an above ground High Explosive Detonation. This shot produces larger particles than a nuclear shot would. Therefore, John modified Sherill's method by using a 100 mesh screen. In

addition, after filtering through the screen, John allowed the mixture to evaporate. Then he took up the residue in water, so that the sample could be analyzed using the Photon Correlation Spectroscopy Equipment. Finally, to check the removal procedure, John weighed beaker and filter paper at the beginning of each Benzene rinse.

John tried this modified method on three different filter paper samples, U-1 blank, Minor Scale, and the archive samples. Preliminary results from the Benzene rinses for each sample are shown in Table XXI. These results indicated that Benzene removes the kronisol after three rinses or with an overnight soak and two one ml rinses. However, two problems occurred with this method. Some of the particles became dislodged from the filter when rinsing with Benzene. If these particles were representative of the total particle distribution, this would not be a major problem. However, if these particles were all at the small or large end of the distribution, then the particles left in the filter would not be a true representation of the particle size distribution. A second problem occurred when the U-1 sample was treated with the ultrasonic probe and filtered though the 100 mesh screen. From preliminary PCS tests it was discovered that the ultrasonic probe creates submicron particles of filter which in turn caused flare to occur in the PCS spectrum. In an attempt to rectify this problem, John tried filtering with a 3 micron Millipore

filter. However, an activity analysis of both the filter and the filtered solution using a small type GeLi detector revealed that up to 90% of the Cs-137 activity (the primary radioactive element in the nuclear sample) was deposited on the filter. From this it was inferred that the three micron filter was catching a significant portion of the particles. Other variations were tried, including heating the solution to try to burn off the fibers, with little success.

TABLE XXI
BENZENE RINSE RESULTS

Sample	Weight of Kronisol Removed (mg)
Blank U-1	12.3
Minor Scale	6.9
Archive	7.3

One variation that could be tried in future experiments would be to place the screen solution in a low temperature asher, to try to oxidize the remaining fibers.

Appendix B: Particle Removal Procedure ("Sherill's" Method)

1. Rinse filter sections in a centrifuge tube containing 35 ml of 65/35 wt% FREON/EtOH mixture.
2. Ultrasonically clean the filters in the 65/35 mix for approximately four minutes with a Branson 350 ultrasonic probe. Repeat three times in separate batches of the 65/35 mix. (Separate batches are required due to heating of the FREON/EtOH mixture during ultrasonification.)
3. Sieve the contents of each centrifuge tube through a 200 m sieve, rinsing the fibers caught on the mesh thoroughly with additional FREON/EtOH mix. Return the sieved mixture plus particles to the centrifuge tubes.
4. Centrifuge all tubes for approximately five minutes at a medium setting.
5. Pipette off the supernatant from each tube being careful not to disturb the particles at the base of the tubes.
6. Rinse the contents of each tube into a single tube with Benzene.
7. Bring up to approximately 35 ml with additional Benzene.
8. Shake this tube well, the purpose of this step being to dissolve off any Kronisol that exists on the surface of the particles.
9. Centrifuge this tube for five minutes at a medium setting.
10. Pipette off the supernatant.
11. Repeat steps 7-10 three times to insure that all

Kronisol is removed.

12. Rinse contents of the tube into a sample vial with Benzene and evaporate to dryness.

Notes:

1. All tests of the above procedure are performed on two 3x2 cm sections of filter at a time.
2. All steps of the procedure are carried out in 50 ml disposable centrifuge tubes.
3. Examination of filter sections under a microscope prior to removing reveals few particles in excess of 100 m in diameter and none that approach 200 m. A slightly coarser sieve can be used if it proves to be necessary.
4. The removal procedure was developed using the Left Pod filter for all trials. Tests of removal efficiency are carried out on the various MS filter samples collected at different levels in the cloud.

INAA Test of Particle Removal Efficiency

The purpose of the following exercise is to determine how well the removal procedure works at removing particles from filters with variable degrees of particle loading. Sc and Fe are used as indicator elements for the presence of particles on the filters as they have relatively long half lives, are ubiquitous in geological materials, and are known to be present at low levels in the filter itself.

Isotopes/Lines:

46Sc / 889.5 KeV T1/2 = 83.8 days

59Fe / 1099.3 KeV T1/2 = 44.6 days

1. A 3x2 cm section is removed from each minor scale filter, including two "sweep" filters which are used as blanks.
2. Each section is irradiated for 8 hours in the L.A.N.L. Omega West reactor at a neutron flux of approximately 10^{11} n cm⁻².
3. The sections are allowed to cool for 20-30 days to allow the activity of other elements in the samples to die down.
4. Each section is counted for 1000 minutes to determine the initial activities of 46Sc and 59Fe. Counts are corrected to DPM at T=0.
5. The removal procedure described above is carried out on each filter.
6. All portions of the cleaned filter are repackaged and counted again on the same detectors at the same geometry for 1000 minutes and again decay corrected to DPM at T=0.
7. Results of the counts are then used to calculate the percentage of particles removed using the equation on the last page of this report.

Notes:

1. The above procedure applies specifically to Minor Scale filter numbers MS1, MS2, MS3, MS7, MS11, and MS12. MS1, a sweep filter, is treated in the same manner as the other

filters and is used as the blank.

2. Minor scale filter numbers MS4, MS5, MS8, MS9, and MS10 are counted at the Omega West reactor for 545 minutes. MS6 is a sweep filter and is used as the blank. The calculation of removal efficiency is performed using net peak areas that are not decay corrected, rather than DPM at $T=0$. The elapsed time between initial and final counts does not exceed one week, thereby introducing negligible errors due to decay between initial and final counts.

TABLE XXII

TABULATION OF INITIAL AND FINAL COUNTS

Sample #	Initial DPM T=0		Final DPM T=0	
	Sc 889.3	Fe 1099.3	Sc 889.3	Fe 1099.3
*MS1	N.D.	3.499 ¹	N.D.	N.D.
MS2	1.130 ²	1.075 ²	7.956	N.D.
MS3	6.008 ²	5.539 ²	2.650 ¹	2.269 ¹
MS7	1.065 ³	8.342 ²	4.419 ¹	4.794 ¹
MS11	1.364 ³	1.257 ³	4.299 ¹	3.285 ¹
MS12	2.554 ³	1.977 ³	8.637 ¹	7.389 ¹

	Initial Net Peak Area		Final Net Peak Area	
	Sc 889.3	Fe 1099.3	Sc 889.3	Fe 1099.3
MS4	4.666 ⁴	1.475 ⁴	1.717 ³	5.280 ²
MS5	4.922 ³	1.226 ³	8.090 ²	N.D.
*MS6	3.250 ²	N.D.	2.060 ²	N.D.
MS8	3.815 ⁴	1.051 ⁴	4.810 ²	1.640 ²
MS9	1.663 ⁴	4.635 ³	8.240 ²	8.600 ¹
MS10	4.990 ³	1.673 ³	3.150 ²	N.D.

* Sweep filter
N.D. Not Detected

TABLE XXIII
PARTICLE REMOVAL EFFICIENCY

Sample #	% Removal 46Sc	% Removal 59Fe
MS2	93.0	N.D.
MS3	95.6	95.6
MS4	96.7	96.4
MS5	86.9	N.D.
MS7	95.9	94.0
MS8	99.3	98.4
MS9	96.2	98.1
MS10	97.7	N.D.
MS11	96.8	97.3
MS12	96.6	96.2

N.D. Not Detected

REMOVAL EFFICIENCY CALCULATION

$$\% \text{ REMOVAL} = [1 - (DPM^{SMP} - DPM^{BLK})_{FINAL} / (DPM^{SMP} - DPM^{BLK})_{INITIAL}] \times 100$$

DPM_{τ₀} = Disintegrations per minute at Time zero.

SMP = Sample

BLK = Blank

Appendix C: PCS Results

No further results were received at the time of this printing.

Appendix D: Sedimentation Field-Flow Fractionation Results

No results were received at the time of this printing.

Appendix E: Abbreviations

A/D	Amplifier/Discriminator
BS	Beam Stop
cc	cubic centimeter
cm	cubic centimeter
FL	Focusing Lens
FS	Field Stop
GeLi	Lithium Drifted Germanium
HV	High Voltage Power Supply
LANL	Los Alamos National Laboratories
LTA	Low Temperature Asher
LV	Low-Voltage Power Supply
ml	milliliter
mg	milligram
N/A	Not Applicable
NBOF	Narrow Band Optical Filter
nm	nanometer
P1	Pinhole 1
P2	Pinhole 2
PCS	Photon Correlation Spectroscopy
PMT	Photomultiplier Tube
POL	Vertically Polarized Light
PPM	Parts per million
QES	Quasi-Electric Light Scattering
S1	Slit 1
S2	Slit 2

AD-A189 718

METHODS FOR DETERMINING PARTICLE SIZE DISTRIBUTIONS
FROM NUCLEAR DETONATIONS(U) AIR FORCE INST OF TECH
WRIGHT-PATTERSON AFB OH C H FORE MAR 87

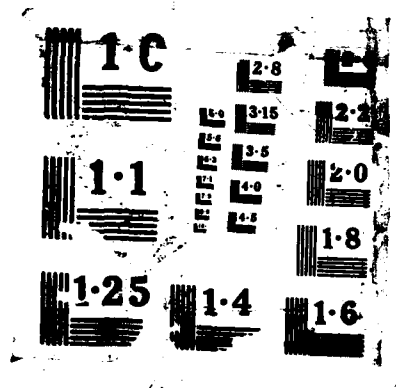
2/2

UNCLASSIFIED AFIT/GNE/PH/87M-2

F/G 18/3

NL





SF³ Sedimentation Field Flow Fractionation
TEM Transmission Electron Microscopy
TL Transmitting Lens
UNK Unknown

Bibliography

1. Barth, Howard G., ed. Modern Methods of Particle Size Analysis. New York: John Wiley and Sons, 1984.
2. Berne, B. J. and R. Pecorn, Ann. Rev. Phys. Chem., 25: 233 (1974).
3. Bevington, Philip R. Data Reduction and Error Analysis for the Physical Sciences. New York: McGraw-Hill Book Company, 1969.
4. Bhatt, J. I. and others. Surface Technology, 15, 323-44, (1982).
5. Bott, S. E. "Submicron Particle Sizing By Photon Correlation Spectroscopy: Use of Multiple Angle Detection," Presented at the American Ceramic Society, May 7, 1985, Cincinnati Convention Center, Cincinnati Ohio, Coulton Reprint No.: T104.
6. Brookhaven Instruments Corporation. BI-2030 Operator's Manual. Publication Date: Unknown.
7. Chu, B. Laser Light Scattering, Academic, New York, 1974.
8. Drake, R. M. and J. E. Gordon. "MIE Scattering," American Journal of Physics, 53:955-962 (October 1985).
9. Freiling, E. C. and G. R. Crocker. Radiochemical Data Correlations For Small Boy: I. Selection, Adjustment and Condensation of Data, Report # NRDL-TR-68-140. San Francisco: U. S. Naval Radiological Defense Laboratory, 1968.
10. Giddings, J. C. and others. "Sedimentation Field Flow Fractionation," Analytical Chemistry, 46: 1917, (1974).
11. Gilder, Jules H. Basic Computer Programs in Science and Engineering. Rochelle Park: Hayden Book Company, Inc., 1980.
12. Gould, Robert F., ed. Radionuclides In The Environment: Advances in Chemistry Series, Washington D. C.: American Chemical Society, 1970.
13. Guinier, Andre and others. Small-Angle Scattering of X-Rays. New York: John Wiley and Sons, Inc., 1955.

14. Happel, J. and H. Brenner. Low Reynolds Number Hydrodynamics. Prentice Hall, Englewood Cliffs, N. J., 1965.
15. Hausner, Henry H. ed. Modern Developments and Processes. Princeton: Metal Powder Industries Federation, 1981.
16. Hollohan, John R., ed. Techniques and Applications of Plasma Chemistry. New York: John Wiley and Sons. 1974.
17. John, George, Personal Interview. Air Force Institute of Technology, Wright-Patterson Air Force Base, OH, 13 November 1986.
18. Kirkland, Jack and Wallace W. Yau. Sedimentation Field Flow Fractionation: A New Method For Characterizing Particulates and Macromolecules. DuPont Instruments, undated.
19. Knobeloch, Gordon, Archive Manager. Personal Interview. Los Alamos National Laboratory, Los Alamos NM, 12 November 1986.
20. McHugh, Anthony J. "Particle Size Measurement Using Chromatography," CRC Critical Review In Analytical Chemistry, 15: 63-117.
21. McWhirter, J. G. and E. R. Pike, J. Phys. A: Math Nucl. Gen., 11:1729 (1978).
22. Malihe, Farrokh B. and others. "Application of Quasi-Elastic Laser Light Scattering For Characterization and Quality Control of Colloidal Dispersions," Journal of Coatings Technology, 55:41-48 (July 1983).
23. Ostrowsky, N., et al. Opt. Acta., 28:1059 (1981).
24. Rundberg, Robert, Staff Scientist, INC-11 Division. Personal Interview. Los Alamos National Laboratories, Los Alamos, N. M., 10 November 1986.
25. Stock, R. S. and W. H. Roy, "Interpretation of Photon Correlation Spectroscopy Data: A Comparison of Analysis Methods," Journal of Polymer Science: Polymer Physics Edition, 23: 1393-1447 (1985).

VITA

Claude Fore was born in Columbus, Ohio, on January 2, 1957. Upon graduation from High School in 1975, he entered the Virginia Military Institute at Lexington, Virginia. He graduated with a Bachelor of Science Degree in Physics in 1979 and was commissioned as an Ordnance Officer in the United States Army. Six years of subsequent Ordnance assignments included 2 years as a Platoon Leader and one year as an Assistant Operations Officer at a Special Weapons Company in Germany. He followed this with a two year assignment as Battalion S-4 at Fort Eustis, Virginia. After departing Fort Eustis, he was assigned to the Air Force Institute of Technology in August of 1985.

Permanent Address: Route 1, Box 375

Lexington, Virginia

24450

ADA189718

REPORT DOCUMENTATION PAGE

Form Approved
OMB No. 0704-0188

1a. REPORT SECURITY CLASSIFICATION UNCLASSIFIED			1b. RESTRICTIVE MARKINGS None	
2a. SECURITY CLASSIFICATION AUTHORITY N/A			3. DISTRIBUTION / AVAILABILITY OF REPORT Distribution Unlimited	
2b. DECLASSIFICATION / DOWNGRADING SCHEDULE N/A			5. MONITORING ORGANIZATION REPORT NUMBER(S)	
4. PERFORMING ORGANIZATION REPORT NUMBER(S) AFIT/GNE/PH/87M-2			7a. NAME OF MONITORING ORGANIZATION	
6a. NAME OF PERFORMING ORGANIZATION Air Force Institute of Technology		6b. OFFICE SYMBOL (if applicable) EN	7b. ADDRESS (City, State, and ZIP Code)	
6c. ADDRESS (City, State, and ZIP Code) Wright-Patterson Air Force Base, Ohio 45433			9. PROCUREMENT INSTRUMENT IDENTIFICATION NUMBER	
8a. NAME OF FUNDING / SPONSORING ORGANIZATION		8b. OFFICE SYMBOL (if applicable)	10. SOURCE OF FUNDING NUMBERS	
8c. ADDRESS (City, State, and ZIP Code)		PROGRAM ELEMENT NO.	PROJECT NO.	TASK NO.
				WORK UNIT ACCESSION NO.
11. TITLE (Include Security Classification)				
12. PERSONAL AUTHOR(S) Fore, Claude H. III				
13a. TYPE OF REPORT Final		13b. TIME COVERED FROM _____ TO _____	14. DATE OF REPORT (Year, Month, Day) 9 March 1987	15. PAGE COUNT 99
16. SUPPLEMENTARY NOTATION				
17. COSATI CODES			18. SUBJECT TERMS (Continue on reverse if necessary and identify by block number)	
FIELD	GROUP	SUB-GROUP	Submicron	
18	03		Particle Size Distribution	
			Photon Correlation Spectroscopy	
19. ABSTRACT (Continue on reverse if necessary and identify by block number)				
Title: METHODS FOR DETERMINING PARTICLE SIZE DISTRIBUTIONS FROM NUCLEAR DETONATIONS				
20. DISTRIBUTION / AVAILABILITY OF ABSTRACT <input checked="" type="checkbox"/> UNCLASSIFIED/UNLIMITED <input type="checkbox"/> SAME AS RPT. <input type="checkbox"/> DTIC USERS			21. ABSTRACT SECURITY CLASSIFICATION UNCLASSIFIED	
22a. NAME OF RESPONSIBLE INDIVIDUAL Fore, Claude H. III			22b. TELEPHONE (Include Area Code) (513) 255-5533	22c. OFFICE SYMBOL AFIT/ENA

Approved for public release: LAW AFB 100-4
14 Sept 87
STAN E. WOLAVER
Dun 161 Research and Professional Development
Air Force Institute of Technology (AFIT)
Wright-Patterson AFB OH 45433

END

DATE

FILMED

APRIL

1988

DTIC